



Contents lists available at ScienceDirect

## Quaternary Science Reviews

journal homepage: [www.elsevier.com/locate/quascirev](http://www.elsevier.com/locate/quascirev)

## Retreat history of the East Antarctic Ice Sheet since the Last Glacial Maximum

Andrew N. Mackintosh<sup>a,\*</sup>, Elie Verleyen<sup>b</sup>, Philip E. O'Brien<sup>c</sup>, Duanne A. White<sup>d</sup>,  
R. Selwyn Jones<sup>a</sup>, Robert McKay<sup>a</sup>, Robert Dunbar<sup>e</sup>, Damian B. Gore<sup>c</sup>, David Fink<sup>f</sup>,  
Alexandra L. Post<sup>g</sup>, Hideki Miura<sup>h</sup>, Amy Leventer<sup>i</sup>, Ian Goodwin<sup>c</sup>, Dominic A. Hodgson<sup>j</sup>,  
Katherine Lilly<sup>k</sup>, Xavier Crosta<sup>l</sup>, Nicholas R. Golledge<sup>a,m</sup>, Bernd Wagner<sup>n</sup>, Sonja Berg<sup>n</sup>,  
Tas van Ommen<sup>o</sup>, Dan Zwartz<sup>a</sup>, Stephen J. Roberts<sup>j</sup>, Wim Vyverman<sup>b</sup>, Guillaume Masse<sup>p</sup>

<sup>a</sup> Antarctic Research Centre, Victoria University of Wellington, PO Box 600, Wellington, New Zealand<sup>b</sup> Ghent University, Protistology and Aquatic Ecology, Krijgslaan 281 S8, 9000 Gent, Belgium<sup>c</sup> Department of Environment and Geography, Macquarie University, NSW 2109, Australia<sup>d</sup> Institute for Applied Ecology, University of Canberra, ACT 2601, Australia<sup>e</sup> Environmental Earth System Science, Stanford University, Stanford, CA 94305, USA<sup>f</sup> Institute for Environmental Research, ANSTO, Menai, NSW 2234, Australia<sup>g</sup> Geoscience Australia, GPO Box 378, Canberra, ACT 2601 Australia<sup>h</sup> National Institute of Polar Research, 10-3 Midori-cho, Tachikawa, Tokyo 190-8518, Japan<sup>i</sup> Department of Geology, Colgate University, Hamilton, NY 13346, USA<sup>j</sup> British Antarctic Survey, Natural Environment Research Council, High Cross, Madingley Road, Cambridge CB3 0ET, UK<sup>k</sup> Department of Geology, University of Otago, PO Box 56, Dunedin, New Zealand<sup>l</sup> Environnement et Paléoenvironnement Océaniques et Continentaux, UMR 5805, Université Bordeaux 1, Avenue des Facultés, 33405 Talence Cedex, France<sup>m</sup> GNS Science, PO Box 30-368, Lower Hutt 5040, New Zealand<sup>n</sup> Institute of Geology and Mineralogy, University of Cologne, Zulpicher Strasse 49a, 50674 Cologne, Germany<sup>o</sup> Australian Antarctic Division and Antarctic Climate and Ecosystems Cooperative Research Centre, Private Bag 80, Hobart 7001, Tasmania, Australia<sup>p</sup> LOCEAN, UMR7159 CNRS/UPMC/IRD/MNHN, Université Pierre et Marie Curie, 4 Place Jussieu, 75252 Paris, France

## ARTICLE INFO

## Article history:

Received 21 December 2012

Received in revised form

2 July 2013

Accepted 17 July 2013

Available online xxx

## Keywords:

Antarctica

Last Glacial Maximum

Ice sheet

Sea level rise

## ABSTRACT

The East Antarctic Ice Sheet (EAIS) is the largest continental ice mass on Earth, and documenting its evolution since the Last Glacial Maximum (LGM) is important for understanding its present-day and future behaviour. As part of a community effort, we review geological evidence from East Antarctica that constrains the ice sheet history throughout this period (~30,000 years ago to present). This includes terrestrial cosmogenic nuclide dates from previously glaciated regions, <sup>14</sup>C chronologies from glacial and post-glacial deposits onshore and on the continental shelf, and ice sheet thickness changes inferred from ice cores and continental-scale ice sheet models. We also include new <sup>14</sup>C dates from the George V Land – Terre Adélie Coast shelf. We show that the EAIS advanced to the continental shelf margin in some parts of East Antarctica, and that the ice sheet characteristically thickened by 300–400 m near the present-day coastline at these sites. This advance was associated with the formation of low-gradient ice streams that grounded at depths of >1 km below sea level on the inner continental shelf. The Lambert/Amery system thickened by a greater amount (800 m) near its present-day grounding zone, but did not advance beyond the inner continental shelf. At other sites in coastal East Antarctica (e.g. Bunger Hills, Larsemann Hills), very little change in the ice sheet margin occurred at the LGM, perhaps because ice streams accommodated any excess ice build up, leaving adjacent, ice-free areas relatively unaffected. Evidence from nunataks indicates that the amount of ice sheet thickening diminished inland at the LGM, an observation supported by ice cores, which suggest that interior ice sheet domes were ~100 m lower than present at this time. Ice sheet recession may have started ~18,000 years ago in the Lambert/Amery glacial system, and by ~14,000 years ago in MacRobertson Land. These early pulses of deglaciation may have been responses to abrupt sea-level rise events such as Meltwater Pulse 1a, destabilising the margins of the ice sheet. It is unlikely, however, that East Antarctica contributed more than ~1 m of eustatic sea-

\* Corresponding author.

E-mail address: [Andrew.Mackintosh@vuw.ac.nz](mailto:Andrew.Mackintosh@vuw.ac.nz) (A.N. Mackintosh).

level equivalent to post-glacial meltwater pulses. The majority of ice sheet recession occurred after Meltwater Pulse 1a, between ~12,000 and ~6000 years ago, during a period when the adjacent ocean warmed significantly. Large tracts of East Antarctica remain poorly studied, and further work is required to develop a robust understanding of the LGM ice sheet expansion, and its subsequent contraction. Further work will also allow the contribution of the EAIS to post-glacial sea-level rise, and present-day estimates of glacio-isostatic adjustment to be refined.

© 2013 Elsevier Ltd. All rights reserved.

## 1. Introduction

This paper describes the changes that occurred in the East Antarctic Ice Sheet (EAIS) during the Last Glacial Maximum (LGM) and subsequent deglaciation, as part of a collective effort by the Antarctic Climate Evolution (ACE) Programme of the Scientific Committee for Antarctic Research (SCAR) to document the behaviour of Antarctica as a whole during this time. The EAIS is the largest ice sheet on Earth, spanning a vast continental area between the longitudes of ~45°W and ~168°E (Fig. 1), exceeding 2 km in thickness over the majority of its area, and reaching a maximum thickness of >4.8 km near its centre (Lythe et al., 2001; Fretwell et al., 2013). It consists of several domes, and is largely separated from the smaller West Antarctic Ice Sheet in the vicinity of the Transantarctic Mountains. Ice retrieved from Dome C in East Antarctica has been continuously dated to 800,000 years old (Parrenin et al., 2007a). Geological evidence shows that an EAIS has probably persisted, with multiple glacial–interglacial cycles, since its initial formation around 34 million years ago (Barrett, 1996).

It is important to understand the Quaternary history of the EAIS for several reasons:

- The EAIS has a volume of  $21.76 \times 10^6 \text{ km}^3$  of grounded ice, equivalent to ~53 m in mean sea-level equivalent (Lythe et al., 2001; Fretwell et al., 2013). Even minor changes in the volume of East Antarctic ice can strongly influence global sea level.
- Ice sheets are one of the key elements of the Earth System. Ice sheets are affected by feedbacks associated with changing atmospheric circulation, planetary albedo and ice elevation (Pollard and DeConto, 2009). They also influence oceanic temperature and circulation through the formation of bottom water, in part beneath ice shelves (Flower and Kennett, 1994).
- Although the EAIS has long been viewed as more stable than the West Antarctic or Greenland Ice Sheets, recent work has cast doubt on this assumption. For example, it may be possible that East Antarctic ice loss contributed to sea-level rise during the Last Interglacial (Pingree et al., 2011).
- The most recent mapping of the bed of the ice sheet (BEDMAP, Fretwell et al., 2013) has now shown that large areas of the EAIS are grounded below sea level and are potentially vulnerable to erosion by ocean currents.
- Present-day observations of ice sheet changes are mostly based on satellite measurements that extend back several decades or less (IPCC, 2007). This period is too short to fully understand natural variability in the ice sheet.
- Deciphering the present-day behaviour of ice sheets using GRACE satellite gravity data requires an understanding of past ice sheet behaviour, because the gravity signal is strongly affected by glacio-isostatic adjustment (GIA) (King et al., 2012).
- The processes governing the response of ice sheets to climate change are imperfectly understood (Joughin and Alley, 2011). Examples of past ice sheet changes provide evidence about where and how fast an ice sheet may respond to environmental forcing.
- Some parts of East Antarctica, especially fast-flowing outlet glaciers (e.g. Totten Glacier, Philippi Glacier) are losing mass at

present, while other, especially slower-flowing areas (e.g. in Enderby Land) appear to be gaining mass (Pritchard et al., 2009; Shepherd et al., 2012). Some ice shelves also appear to be losing considerable mass from sub-shelf melting and not just calving (e.g. Totten Ice Shelf, West Ice Shelf) (Rignot et al., 2013). The long-term ice sheet history in these areas might aid in understanding recent ice sheet behaviour.

- Antarctica may have been one of the sources of abrupt sea-level rise events during deglaciation known as ‘meltwater pulses.’ In particular, an Antarctic contribution has been inferred for Meltwater Pulse 1a (MWP1a) (Clark et al., 2002; Deschamps et al., 2012). Discussion and further study of the geological evidence from East Antarctica is needed in order to identify or rule out possible sources of meltwater pulses.

## 2. Aims

We aim to describe the marine and terrestrial geological evidence that constrains the history of the EAIS immediately prior to, during and following the LGM. Our specific objectives are to:

1. Summarise evidence for past ice thickness and extent using onshore and offshore records.
2. Compile a table of robust age constraints for glacial features (with an assessment of quality control). This table is available as [Supplementary material](#).
3. Discuss the implications of our findings for understanding the response of the ice sheet to past climate changes, including its possible contribution to global meltwater pulses.

## 3. Study regions and data sources

The LGM glacial history of East Antarctica is poorly documented (Ingólfsson et al., 1998; Bentley, 1999; Wright et al., 2008). Relatively little of the continental shelf surrounding East Antarctica has been studied (Anderson et al., 2002; Livingstone et al., 2012), and although deglaciated regions occur at both the ice sheet margin and further inland, only a few previous studies provide strong constraints on their glacial history. Ice cores from the interior as well as Law Dome near the ice sheet margin also provide some constraints on past ice sheet thickness (Fig. 1, Table 1).

Ice-free regions, known as ‘oases’, occupy a small percentage of the overall land area in Antarctica (Fig. 1). Oases typically occur in coastal areas adjacent to large outlet glaciers. Ice-free regions also occur within mountain ranges or on individual mountain nunataks, which extend into the ice sheet interior. We describe the geomorphology of each of these regions, focussing on the features that constrain the maximum ice extent during the LGM and the chronology of deglaciation. For ice sheet chronology, we report only absolute dating methods: Radiocarbon ( $^{14}\text{C}$ ), Terrestrial Cosmogenic Nuclide (TCN) and Luminescence (Optically Stimulated Luminescence – OSL, Infrared Stimulated Luminescence – IRSL) dating. All dates referred to in the text are provided in a [Supplementary data](#)



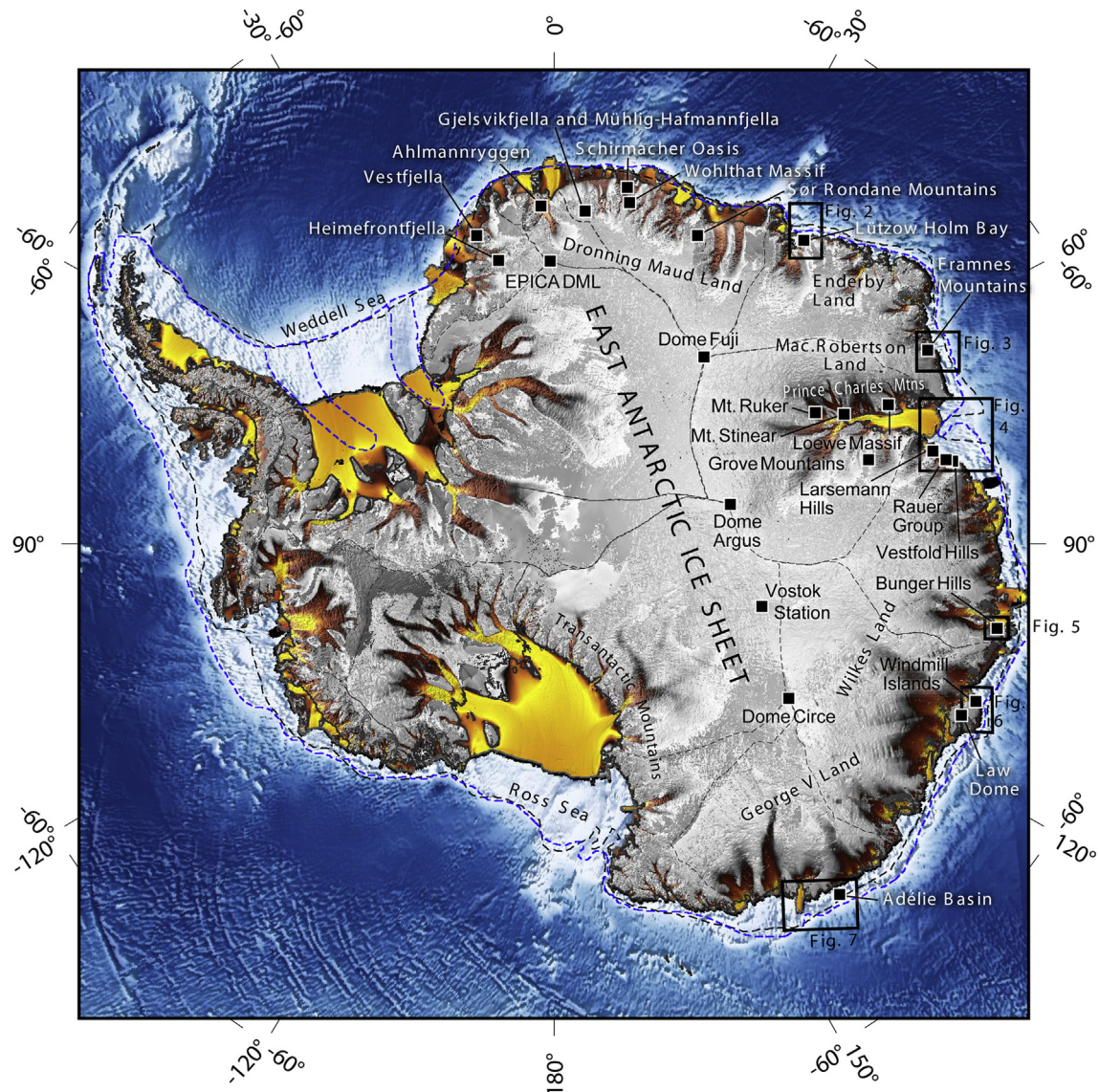


**Fig. 1.** Map of Antarctica showing locations mentioned in the text. This review covers the East Antarctic Ice Sheet, excluding the Ross and Weddell Embayments. Boxes show the marine regions covered in Figs. 2–7. The ice sheet is shaded in grey hues where it is of high relief and slow moving, and ice divides are marked. Fast moving ice streams and ice shelves (>1 km/yr in places) are shown in bright orange and yellow colours (Rignot et al., 2011). Continental shelf areas are indicated by white hues, and the deeper ocean is blue. Estimated LGM grounding zone positions are from Anderson et al. (2002) (black line) and Livingstone et al. (2012) (blue line).

table, with the exception of TCN ages, which clearly contain a signal of inheritance, or significantly pre-date the LGM.

The most direct chronological terrestrial evidence of EAIS history comes from TCN dating of moraines, erratic boulders and ice-

abraded bedrock surfaces (Balco, 2011). Developing a chronology using this method in polar settings can be challenging, as ice that overran presently ice-free areas during the LGM often eroded little sediment or bedrock, particularly under cold-based ice. This lack of

**Table 1**

Ice elevation changes from the interior of the EAIS, based on ice core records (Fig. 1) and ice sheet models. Sites from the East Antarctic interior dominantly show ice surface lowering at the LGM, while Law Dome (a coastal site, Fig. 1) mostly shows thickening. Ice core estimates marked by an asterisk are based on a 1-D ice flow model specific to each ice core site, derived using an analytical velocity profile, taking into account variations in ice thickness and deducing the accumulation rate from the isotopic content of the ice (Parrenin et al., 2007b). Note that this type of ice model is highly tuned with ice core data and differs markedly from continental-scale ice models (e.g. Golledge et al., 2012; Whitehouse et al., 2012). Data from Mackintosh et al. (2011) are from a high-resolution (20 km) version of the Pollard and DeConto (2009) ice sheet model. Estimates for Vostok (Lorius et al., 1984) and Law Dome (Delmotte et al., 1999) are derived from total gas content.

| Ice core | Surface elevation change inferred from ice core (m) | Mackintosh et al. (2011) surface elevation change (m) | Golledge et al. (2012) surface elevation change (m) | Whitehouse et al. (2012) surface elevation change (m) |
|----------|---|---|---|---|
| Dome C   | –120*   | –124  | –106  | –105  |
| Vostok   | ~100  | –103  | +112 (increase)                                     | –143  |
| Dome F   | –120*   | –126  | –206  | –112  |
| EDML     |   | –95   | –375  | –163  |
| Law Dome | 136–335 (increase)                                  | 144 (increase)  | –171  | 356 (increase)  |

geomorphic effectiveness means that glacial deposits are often a mixture of material sourced from rock well shielded from cosmic rays, and sediment or bedrock that has been reworked from a period of prior exposure. Hence the most recent glacier or ice sheet advance may deliver a mixture of erratic boulders whose TCN represents the timing of the last advance, along with a population that considerably over represents the true deglaciation age. Although there are no strict guidelines, where independent evidence is lacking, most scientists choose an age model based on the younger ages for a given elevation within a sequence, and exclude age populations that are anomalously old for the site (Stone et al., 2003; Mackintosh et al., 2007). At some sites the analysis of two or more isotopes allow cosmogenic inheritance and/or burial to be identified (Bentley et al., 2006; White et al., 2011a), which reduces ambiguity in the interpretation of deglaciation timing from a population of erratics. However, in some areas suitable lithologies for TCN are not available. In addition to these geological and geomorphological issues, there has been a re-assessment of commonly used AMS standard reference materials which directly impacts on sea level high latitude calibration isotope production rates (Fink and Smith, 2007; Nishiizumi et al., 2007). TCN ages reported in the text and the Supplementary data table have been re-calculated using the on-line CRONUS calculator (Balco, 2009), which guarantees a uniform and consistent application of various production rate and scaling factors. Input concentrations and all other necessary information has been carefully extracted from the cited publications and made self-consistent with CRONUS data input requirements. TCN ages are reported as 'years ago' (yr ago) or kiloyears ago (ka ago), where the reference date is the year that the sampling was carried out.

Radiocarbon dating in terrestrial areas can only be used to date organic or carbonate material that provides an indirect and usually a minimum constraint on ice sheet history. Typically, this involves dating of the bulk carbon, or the carbon contained in discrete macrofossils, deposited in lake and terrestrial sediments formed after deglaciation. Extracted fractions of the Acid Insoluble Organic Matter (AIOM) can also be used to reduce errors associated with multiple carbon sources. Other organic material can also provide minimum ages for deglaciation, such as snow petrel (*Pagodroma nivea*) stomach ejecta known as *mumiyo* (Verkulich and Hiller, 1994), which forms layered deposits on bedrock sites. Marine macrofossils such as shells, seal hairs, penguin feathers and bones deposited are often found within raised beaches. In some of the cases mentioned above, a marine reservoir correction (Reimer and Reimer, 2001) is required despite the terrestrial setting, particularly when the 'terrestrial' material is sourced from the marine environment. For example, snow petrels feed from the ocean, and marine shells can be found in fossil beaches. Further information is provided below. In terrestrial environments, luminescence dating of raised beaches, fluvial and lacustrine deposits can sometimes provide a useful supplement to radiocarbon dating, but usually with larger errors (Gore et al., 2001; Simms et al., 2011).

For marine evidence, we discuss the glacial geomorphology of the continental shelf region where bathymetric evidence is available, and focus on radiocarbon dating of glacial and deglacial facies in marine sediment cores. Much of the East Antarctic continental margin has not been studied so that the marine record is limited to three areas of intense study and two areas where limited study has taken place or the studies involve records from the continental slope. These latter studies are valuable for timing of regional deglaciation but do not constrain grounding-line positions or retreat chronology. The three areas of major study are the Mac-Robertson Land shelf, Prydz Bay and the George V Land – Terre Adélie Coast shelf (Fig. 1).

The East Antarctic shelf has a geomorphology typical of a glaciated continental margin with inner-shelf deeps, outer-shelf

banks and cross-shelf troughs. Selective glacial erosion is evident in the great overdeepening of inner shelves, often reaching >1000 m. The shelf break typically occurs at around 400–500 m water depth. Outer banks are generally 100–200 m deep. Shelf geomorphology affects the advance and retreat of the ice sheet. In some areas, the LGM ice sheet expanded to the continental shelf edge, filling the inner-shelf basins and troughs. In such places, the spatial extent of the ice sheet advance is recorded by streamlined bedforms such as Mega Scale Glacial Lineations (MSGs) (Clark, 1993; Livingstone et al., 2012) and Grounding Zone Wedges (GZWs) (Dowdeswell and Fugelli, 2012), which mark the transition between formerly grounded and floating ice on the continental shelf. In other locations, the ice sheet appears not to have expanded beyond the innermost-shelf, and may have had similar dimensions to the current ice sheet margin at the LGM.

The retreat history of the ice sheet is often well recorded in sediment deposited in shelf troughs. Typically, these deposits are recovered via gravity or jumbo piston coring. Sediment cores for the most part show a transition from ice-proximal sediment such as till or diamict at the base to a diatom-rich ooze. At many locations, rhythmically laminated sediment couplets are preserved near the transition between till and diatom ooze. These deposits have been interpreted as ice-proximal sediment couplets, interpreted as 'calving bay' (Hughes, 2002) sediments, deposited in fjord-like embayments bounded by ice on their margins. They often form a particularly useful constraint on the timing of ice retreat, because they represent the onset of deglaciation, when significant ice remained on the outer-shelf banks (Leventer et al., 2006).

For each sediment core, we discuss the geological facies present and the quality of the dating control. In many cases,  $^{14}\text{C}$  dates from marine cores are affected by the recycling of old carbon (Gordon and Harkness, 1992; Andrews et al., 1999). We therefore focus on sites where (1) ages fall in correct stratigraphic order, (2) it is possible to date discrete macrofossils, not just AIOM and (3) facies associations provide strong evidence about the proximity of the ice, or post-depositional reworking by bioturbation or current winnowing. Site-specific marine reservoir age corrections are required in all Antarctic marine settings but were only used in a few cases (as noted in the text, e.g. at IODP site U1357 in the Adélie Basin), where convincing core-top radiocarbon dates were available to provide the modern surface age correction. The justification for core-top corrections of AIOM dates is based on the assumption that input of "old" carbon is constant through time, and therefore this correction can only be applied if there is no change in sedimentary depositional environment, and as such corrections can only be reliably made at the onset of open marine deposition at any given site (c.f. Ross Sea studies of Domack et al. (1999), McKay et al. (2008)). Significant changes in sedimentation rate or bioturbation may also provide additional indicators that sediment input was not constant through time (Domack et al., 1999). Nevertheless, core-top corrected ages from AIOM marine dates are often considered more reliable than applying a uniform 'Antarctic' marine reservoir correction, but both should be treated with caution, especially if no paired dates on marine macrofossils are present.

By convention, radiocarbon ages are reported as years 'Before Present' (yr BP) or kiloyears 'Before Present' (ka BP), where 'present' is defined as AD 1950. Uncalibrated and uncorrected  $^{14}\text{C}$  dates are referred to by including ' $^{14}\text{C}$ ' before years in the quoted age. Calibrated (cal) ages were calculated using the programme Calib 6.1.1 (Stuiver and Reimer, 1993), and we report the 2-sigma age ranges. For marine radiocarbon ages or ages from terrestrial sites with a predominantly marine influence, we use the Marine09 calibration curve (Reimer et al., 2009), applying a uniform 'Antarctic' marine reservoir correction of  $1300 \pm 100$  years (Berkman and Forman, 1996), unless otherwise stated. Calib 6.1.1 includes a default



marine reservoir correction of 400 years, so we add an additional  $900 \pm 100$  years to account for a total correction of  $1300 \pm 100$  years.

For terrestrial dates with no marine influence (e.g. from lacustrine macrofossils), we use the SHCal04 curve (McCormac et al., 2004), unless samples exceeded its age range ( $\sim 11$  cal ka BP), in which case we apply the IntCal09 curve (Reimer et al., 2009). When generalising, we report median calibrated  $^{14}\text{C}$  ages rounded to the nearest thousand years. We also note where  $^{14}\text{C}$  ages are likely to be infinite, and thus provide only a minimum estimate of the true deglaciation age.

We also discuss evidence for changes in ice sheet thickness and extent from the ice sheet interior, focussing on ice cores and constraints from recent continental-scale ice sheet models.

#### 4. Review of Last Glacial Maximum evidence

##### 4.1. Dronning Maud Land

Unlike other East Antarctic regions, the ice sheet in a vast sector of Dronning Maud Land (DML) is dammed by mountain chains, which run from the Borg Massif in Western DML ( $5^\circ\text{W}$ – $73^\circ\text{S}$ ) to the Yamato Mountains in the east ( $35^\circ\text{E}$ – $72^\circ\text{S}$ ) (Pattyn et al., 2010). This results in steep slopes from the continental plateau (i.e. the EAIS south of the nunataks) towards the lower coastal ice masses. Till and striated bedrock are present in these mountains, together with lake sediments and organic deposits, such as mumiyo, which provide evidence for past changes in the dynamics and extent of the EAIS. Below we describe the nunataks and mountain ranges in DML from west to east for which the deglaciation history has been (partially) reconstructed.

##### 4.1.1. Vestfjella and Heimefrontfjella

The Vestfjella and Heimefrontfjella mountain ranges in west DML (Fig. 1) run approximately parallel with the present coastline. Vestfjella is  $\sim 130$  km long and is situated 120 km from the coast. The glaciers surrounding the nunataks drain into the Riiser-Larsen Ice Shelf in the Weddell Sea and the highest elevation in the region is  $\sim 1100$  m above sea level (asl) (Lintinen, 1996). The Heimefrontfjella range,  $\sim 150$  km further inland from Vestfjella, is  $\sim 150$  km long with elevations up to 2600–2700 m asl. The deglaciation history of Vestfjella and Heimefrontfjella was reviewed in Lintinen (1996) and Hattestrand and Johansen (2005), but chronological controls and constraints on past extent remain limited. Jonsson (1988) reported striae and till on nunataks in Vestfjella, and concluded that the ice sheet did not cover the higher peaks of the mountain range. In contrast, Lintinen (1996) and Lintinen and Nenonen (1997) reported basal till and glacial striae on most nunataks in Vestfjella. Hence, the whole range was probably overridden by the EAIS at some point. Based on the generally unweathered appearance of these tills, Lintinen (1996) speculated that they were deposited during the LGM ice sheet expansion. However, no dates are available to confirm or reject this hypothesis. If correct, this implies that in Vestfjella the ice sheet during the LGM must have been at least 700 m thicker than today (i.e. 1100 m asl) (Hattestrand and Johansen, 2005). Radiocarbon dates of mumiyo deposits revealed that some areas in the region were ice free since at least  $38,700 \pm 1500$   $^{14}\text{C}$  yr BP (Thor and Low, 2011) ( $39,098$ – $44,358$  cal yr BP; most likely an infinite age).

In Heimefrontfjella (Fig. 1), evidence for two former limits of glaciation is preserved (Patzelt, 1988). The lower limit is 100–150 m above the present ice surface and contains a large number of unweathered erratics compared with the upper zone, which is up to 430 m above the present ice surface. Lintinen and Nenonen (1997) noted that the weathering of the regolith on surfaces in the lower

zone was as weakly developed as in Vestfjella. From this, they concluded that the ice sheet during the LGM was up to 100–200 m thicker than today. However, in common with Vestfjella, there is no chronological control available. A minimum age of deglaciation based on  $^{14}\text{C}$  dates of the basal layers of low lying snow petrel nests (30–230 m above the present ice surface) suggests that the ice surface must have been below 30 m above present since at least  $8700 \pm 40$   $^{14}\text{C}$  yr BP (Lintinen and Nenonen, 1997) ( $8015$ – $8471$  cal yr BP). Based on the analysis of a marine sediment core from the Weddell Sea, Elverhoi (1981) suggested that a grounded ice sheet was present more than 100 km beyond the present-day grounding zone immediately seaward of this region, probably around 21 ka BP.

##### 4.1.2. Ahlmannryggen, Gjelsvikfjella, and Wohlthat Massif

Ahlmannryggen (Fig. 1) is a mainly ice covered ridge in west DML,  $\sim 70$ – $100$  km from the ice sheet margin, and comprises a series of small and scattered nunataks with a maximum elevation of 1843 m asl (Neethling, 1969). The ridge is situated between glaciers which drain into the Fimbul Ice Shelf along Princess Martha Coast. Glacial deposits from this ridge suggest that the ice sheet did exceed 1160 m asl at a distance of 250 km from the outer ice sheet margin (Neethling, 1969).  $^{14}\text{C}$  dates on mumiyo deposits sampled over an altitudinal gradient from the foot to the summit of several nunataks are all of Holocene age, with the oldest date of  $8330 \pm 70$   $^{14}\text{C}$  yr BP ( $7652$ – $8149$  cal yr BP) providing a minimum age for deglaciation (Steele and Hiller, 1997). However as this is a minimum age of exposure, it is possible that the summits escaped glacial overriding during the LGM.

Gjelsvikfjella (Fig. 1) and the western part of Mühlig-Hafmannfjella (Fig. 1) are 220–200 km from the outer ice sheet margin, with maximum elevation ranges of between 2700 and 3020 m asl (Engelskjøn, 1986). In Gjelsvikfjella the mumiyo deposits so far analysed are of Holocene age with the oldest date being  $3730 \pm 80$   $^{14}\text{C}$  yr BP (Steele and Hiller, 1997) ( $2268$ – $2871$  cal yr BP). By contrast, mumiyo deposits sampled close to the present-day ice sheet (at 1610 m asl) in the Svarthamaren nunatak in the western part of Mühlig-Hafmannfjella are  $28,150 \pm 420$  and  $33,820 \pm 1700$   $^{14}\text{C}$  yr BP old (Steele and Hiller, 1997) ( $30,542$ – $31,962$  and  $33,809$ – $41,098$  cal yr BP respectively). This suggests that the EAIS in this region has remained close to its present position since before the LGM or significantly longer if these  $^{14}\text{C}$  dates are infinite ages.

Schirmacher Oasis (Fig. 1) is an ice-free area, with numerous lakes and ponds and a maximum elevation of 228 m, situated between the EAIS and the Nivl Ice Shelf (Lazarev Sea). The present-day geomorphology is the result of glacial erosion and characterised by low relief hills and linear valleys (Richter and Bormann, 1995). Dates from lake sediments based on IRSL yield conflicting information (Krause et al., 1997). Two cores from Lake Glubokoye revealed significant age reversals from top to bottom and should be discounted. The remaining core from Lake Dlinnoye revealed ages of  $\sim 24$  ka BP at the base  $\sim 1.30$  m, and 7 ka BP at 0.87 m depth. Thermoluminescence age estimates were inconsistent with those derived from IRSL (Krause et al., 1997). While these IRSL ages are problematic, they are broadly consistent with the pre-LGM  $^{14}\text{C}$  determinations on the lake sediments (Krause et al., 1997). These chronologies suggest that some of the lakes at Schirmacher Oasis may have been ice free before the LGM, although we note that this remains to be verified by further dating. A hiatus at the Holocene sediment base in sediment cores from Lake Zub and Lake Glubokoye suggest that the region was overridden by the EAIS during the LGM (Schwab, 1998). This is consistent with basal sediments in subaerial lake sediment profiles near Long Lake which date to  $12,900 \pm 70$   $^{14}\text{C}$  yr BP ( $15,016$ – $16,099$  cal yr BP) (Phartiyal et al.,

2011). This, however, postdates estimates based on TCN dating of bedrock, which revealed that the region was ice-free before the LGM (i.e., >~35,000 years ago) (Almaier et al., 2010), although supporting TCN dates from erratic boulders are required to test this hypothesis. An early Holocene deglaciation of the continental shelf in the Lazarev Sea was inferred from a  $^{14}\text{C}$  date of  $11140 \pm 120$   $^{14}\text{C}$  yr BP (10789–11876 cal yr BP) on laminated sediments near the Nivl Ice Shelf (Gingele et al., 1997). After deglaciation, large proglacial lakes developed in Schirmacher Oasis, which subsequently evolved into the present landlocked lakes at ~3 ka BP as a result of excess ablation or the recession of glaciers in their catchment area (Phartiyal et al., 2011).

The Wohlthat Massif (Fig. 1) is situated ~100 km further to the south of Schirmacher Oasis and consists of the Peterman Range, Gruber Mountains and Humboldt Mountains (Kämpf et al., 1995). The nunataks reviewed here are the Insel Range and the Untersee Oasis (Hiller et al., 1995) and have a maximum elevation of ~2855 m. TCN dates suggest that only minor changes in ice sheet thickness occurred over the past 100,000 years, implying that the EAIS did not advance significantly during the LGM in this region (Almaier et al., 2010). This is supported by a  $^{14}\text{C}$  date of  $32,480 \pm 740$   $^{14}\text{C}$  yr BP on mumiyo deposits in the Insel range (34,478–37,407 cal yr BP), which provides a minimum age that snow petrels were present in locations up to 50 m above the present-day ice sheet (i.e. at ~1470 m asl) (Hiller et al., 1995). Near Lake Untersee the ice sheet was below 950 m asl a few tens of thousands of years or longer before the LGM ( $33,900 \pm 3020$   $^{14}\text{C}$  yr BP; 31,322–42,598 cal yr BP; minimum age). By  $8020 \pm 180$   $^{14}\text{C}$  yr BP (7228–8000 cal yr BP) the ice sheet was below 700 m asl (Hiller et al., 1988). The  $^{14}\text{C}$  dates near Lake Untersee may be infinite ages and thus provide only a minimum constraint on the timing of glaciation. Hence it is very likely that the EAIS did not change much in this region during the LGM.

#### 4.1.3. Sør Rondane Mountains

The Sør Rondane Mountains (Fig. 1) trend east–west and are the most southerly mountain range in central Dronning Maud Land. They are 220 km long, situated 200 km from the coast and have a maximum elevation of ~3000 m (Pattyn et al., 2010). The region holds one of the best-preserved moraine sequences of DML (Moriwaki et al., 1991). Similar to the Wohlthat Massif, early TCN dates suggest that although large parts of the elevated inner Sør Rondane Mountains have remained ice-free for at least the past 4 million years, more peripheral nunataks only became ice-free more recently (<200,000 years ago). Moriwaki et al. (1991) and Moriwaki et al. (1992) divided the glacial history of the Sør Rondane area into five stages based on weathering evidence, and subsequently, TCN dating of exposed bedrock (Nishiizumi et al., 1991; Ishizuka et al., 1993), with the final stage occurring with the last 25 ka and characterised by thin, supraglacial moraine fields within 100 m and 30 m above the present ice surface (Moriwaki et al., 1992). In other words, the available TCN dates suggest that the EAIS did not exceed 100 m above its present-day elevation (Matsuoka et al., 2006) during the LGM.

#### 4.1.4. Lützow-Holm Bay

The ice-free regions in Lützow-Holm Bay (Figs. 1 and 2) form a north-south oriented coastal oasis along the margins of eastern Dronning Maud Land. Glacial striae and scattered erratic boulders are found on all of the major ice-free islands and peninsulas. The geomorphology is characterized by low-relief hills which have been shaped by glacial erosion. The highest elevation is 497 m, with raised beaches, emerged marine deposits and numerous lakes all occurring in the region.

In Lützow-Holm Bay,  $^{14}\text{C}$  ages of fossil shells in raised beaches can be classified into either Holocene (<7 ka BP) ages or pre-

LGM (~33–50 ka BP) ages (Miura et al., 1998a; Takada et al., 2003) (Fig. 2) (Supplementary data table). However,  $^{14}\text{C}$  dates in 17 marine sediment cores from the Lützow Holm Bay region are all younger than ~16 ka BP (Igarashi et al., 2001), although the oldest dates are derived from glaciomarine sands and gravels and likely have a substantial reworked carbon component, and some may be infinite ages. Fossils of Holocene age occur on all islands studied so far. By contrast, the late Pleistocene fossils are restricted to the northernmost part of Sôya Coast, namely East and West Ongul islands and the northern part of Langhovde (Fig. 2). There, the presence of Pleistocene *in situ* shells of the fragile bivalve *Laternula elliptica* suggests that the EAIS had retreated at least from the Ongul Islands and the northern part of Langhovde by 30–46 ka BP, and did not readvance over this region during the LGM. An alternative hypothesis is that the LGM ice sheet was non erosive over the region which resulted in the *in situ* preservation of the marine fossils, though this is unlikely due to the fragile nature of the *Laternula elliptica* shells and the fact that they are preserved in their original ‘feeding’ position. The lack of late Pleistocene marine fossils in Skarvsnes and Skallen (Fig. 2) suggest that the EAIS retreated from these regions after the LGM. This is confirmed by a recent TCN dating campaign, which suggest that the ice sheet in Skarvsnes (Fig. 2) was at least 360 m thick and that the peninsula became ice-free between 10 and 6 ka ago (Yamane et al., 2011). These differences in deglaciation history are confirmed by the relative amount of weathering of the surface rocks. Rocks in the northernmost part of Sôya Coast are deeply weathered, whereas those in the southern part of coast (i.e. Skarvsnes and Skallen) are relatively unweathered and intensively striated (Miura et al., 1998b).

#### 4.2. Mac.Robertson Land

In Mac.Robertson Land, deglaciation chronologies are available both onshore (Framnes Mountains) and on the adjacent continental shelf (Iceberg Alley and Nielsen Basin) (Fig. 3). Together, this geological evidence provides one of the most complete records of ice extent and the timing of deglaciation in East Antarctica. Although the Prince Charles Mountains technically lie in Mac.Robertson Land, they are reviewed in the Lambert/Amery section because they constrain the ice sheet history of this large outlet glacier system.

##### 4.2.1. Framnes Mountains

The Framnes Mountains comprise a chain of nunataks that extend from 10 to 50 km inland of the coast of Mac.Robertson Land (Figs. 1 and 3). The mountains reach an elevation of ~1500 m asl, and protrude up to 400 m above the present ice-sheet surface. Dark-coloured, weathered charnockite bedrock in Framnes Mountains is littered with light-coloured quartz-rich, granitic gneiss glacial erratics, indicating widespread thickening and in some cases overriding of the mountains by an expanded ice sheet during the late Quaternary (Mackintosh et al., 2007). The erratics lie on bedrock that shows evidence of prolonged surface exposure, such as weathering pits and tafoni. This suggests that cold-based ice was prevalent during the last overriding of these mountains. The scale of ice sheet thickening, marked by the upper limit of glacial erratic boulders, diminishes inland, ranging from ~400 m within 10 km of the coast (Mt. Henderson) to ~160 m at around 50 km inland (Brown Range) (Mackintosh et al., 2007). This upper limit of boulders is also traceable along the length of the David Range at a gradient that is similar to the present-day ice sheet surface. This boulder limit reduces from ~1300 m asl on Mt Hordern, approximately 30 km inland from the coast, to 1100 m on Mt Coates, 860 m on Mt Elliott and 820 m on Fang Peak, a further 15 km seaward.

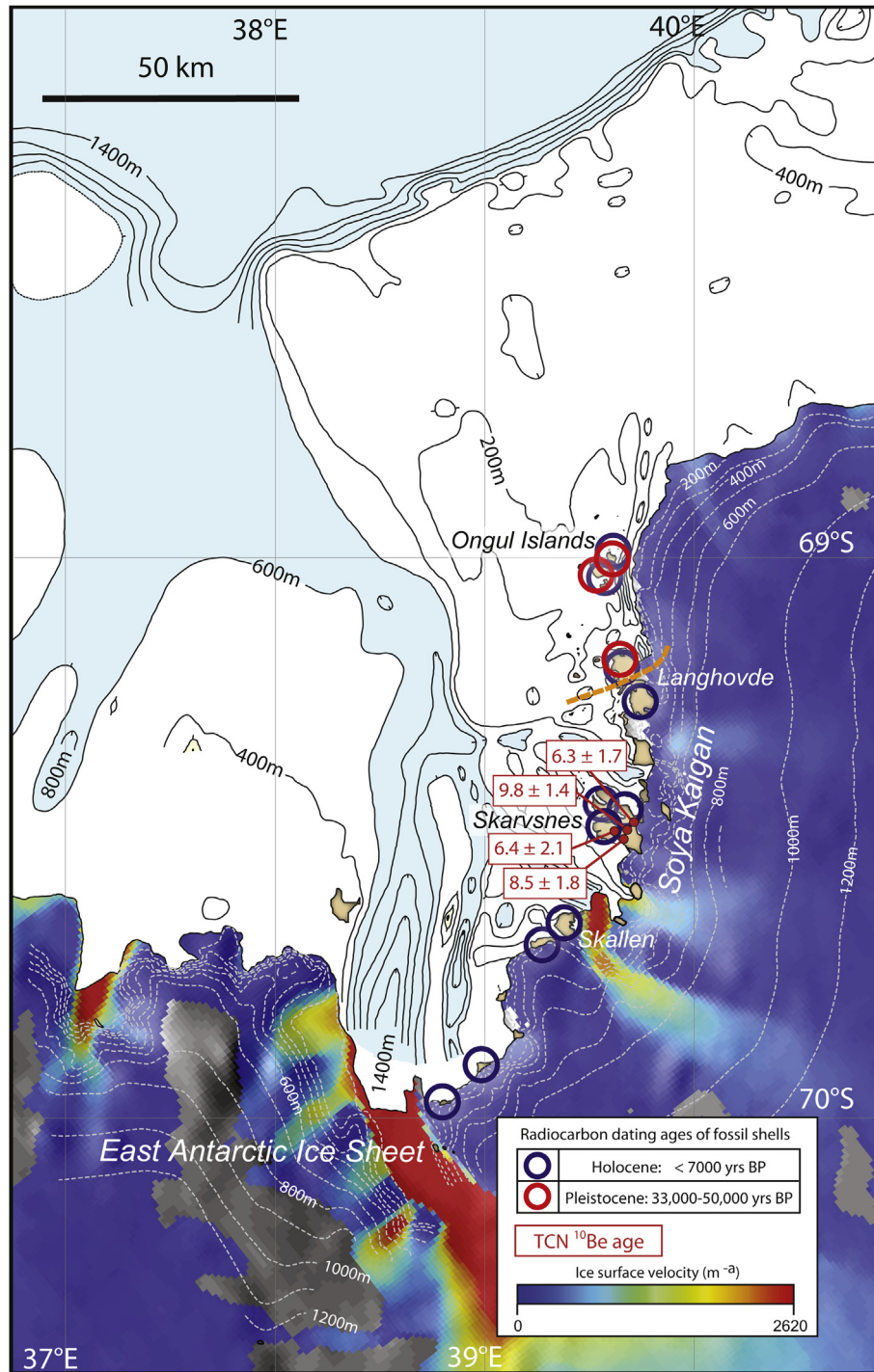


**Fig. 2.** Map of Lützow-Holm Bay, Dronning Maud Land. Ice sheet velocity is shown (Rignot et al., 2011), as is the generalised offshore bathymetry (detailed swath mapping has not been carried out). Coastal ice-free areas and dating sites are highlighted. The southern peninsulas of Skarvsnes and Skallen became ice free during the Holocene, whereas areas north of the dashed line may have remained ice free throughout the LGM.

Glacial erratics have been sampled for TCN ( $^{10}\text{Be}$  and  $^{26}\text{Al}$ ) analyses from summit level to the modern ice sheet surface. The ages indicate 350–400 m lowering of the ice sheet surface occurred near the present coast between the LGM and the mid Holocene (Mackintosh et al., 2007). Ages from the North Masson Range show that ~200 m lowering occurred between ~12 and ~10 ka ago. Supporting dates from Mt. Henderson, Central Masson and David Ranges indicate that a further 200 m of surface lowering took place between ~9 and ~7 ka ago (Mackintosh et al., 2007). The youngest

cosmogenic ages from boulders located <10 m above the ice surface indicate that the present-day ice sheet profile was attained by ~7 ka ago. Further inland at Brown Range (~50 km from the coast), TCN ages decrease from ~23 ka at the summit to ~1 ka at the present day ice margin, although the small sample size ( $n = 4$ ) means the interpretation of the Brown Range TCN ages is less secure than for the ranges closer to the coast (Mackintosh et al., 2007).

The TCN data used to constrain ice histories in the Framnes Mountains have been corroborated by independent evidence. For



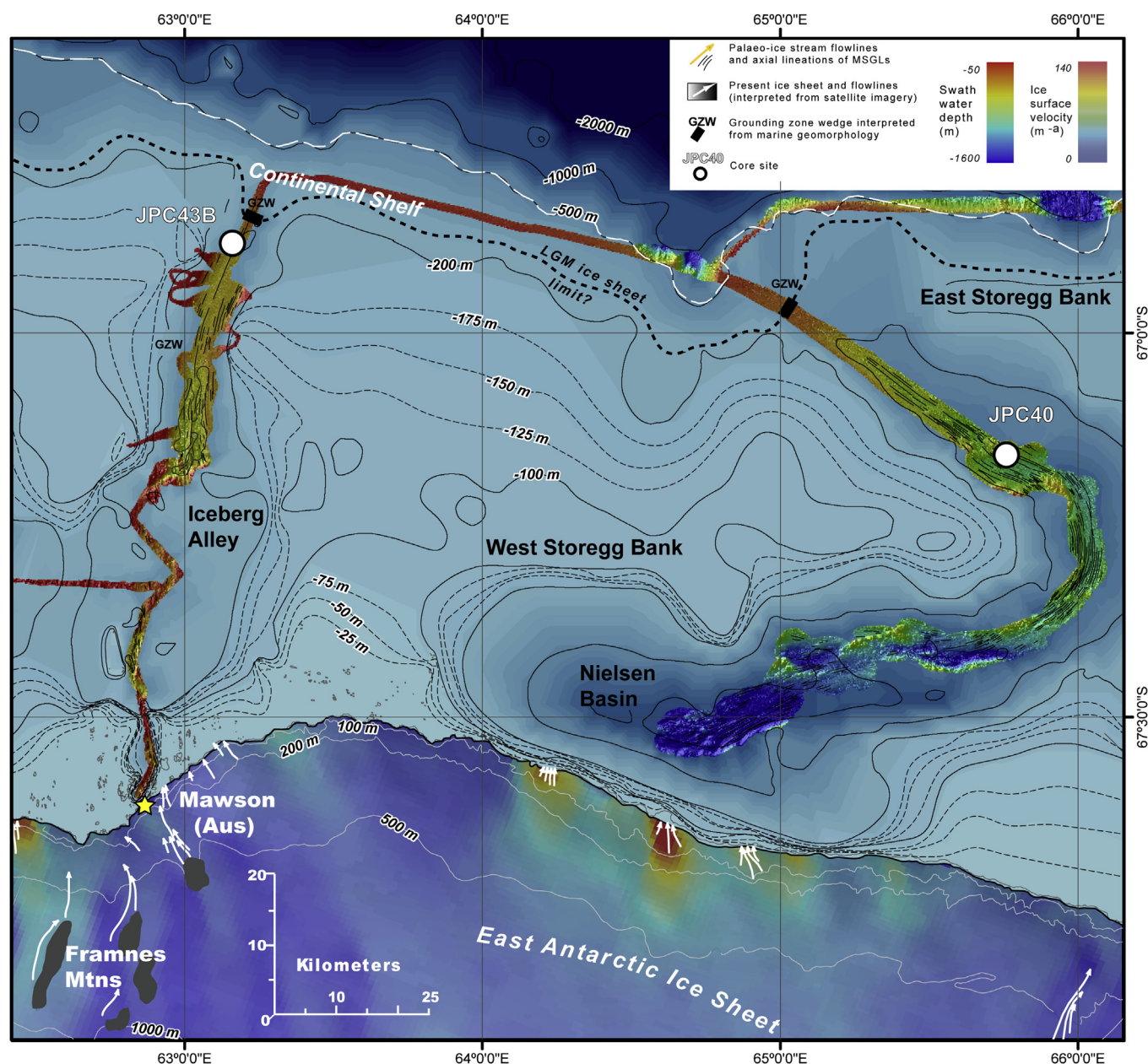


**Fig. 3.** Map of Mac.Robertson Land, showing the location of Framnes Mountains (onshore), Iceberg Alley (including core JPC43B), Nielsen Basin (including core JPC40), streamlined bedforms, grounding zone wedges, and the continental shelf margin. Shelf bathymetry and the interpreted LGM grounding zone (Mackintosh et al., 2011) are also shown, as is ice velocity (Rignot et al., 2011).

example,  $^{14}\text{C}$  dating of mumiyo deposits from the North Masson Range indicates that bedrock near the present ice margin was ice free by  $7103 \pm 48$   $^{14}\text{C}$  yr BP (6391–6915 cal yr BP), consistent with the youngest TCN dates from this site (Mackintosh et al., 2011). Further, three erratics from the David and North Masson Ranges have been dated using *in-situ*  $^{14}\text{C}$  (a TCN) and indicate that the younger population of erratics used to constrain ice histories contain negligible inherited  $^{10}\text{Be}$  and  $^{26}\text{Al}$  (White et al., 2011a).

#### 4.2.2. Mac.Robertson Land continental shelf

The Mac.Robertson Land continental shelf extends ~80 km seaward of the present-day ice sheet margin (Fig. 3). Two prominent cross-shelf troughs, Nielsen Basin and Iceberg Alley, dissect the shelf (Leventer et al., 2006). MSGs in both troughs reflect the presence of formerly streaming ice, and indicate ice sheet

grounding occurred to >1 km below modern-day sea level (Mackintosh et al., 2011). In Iceberg Alley, ice streaming occurred preferentially in the deeper part of the trough, from the mid- to outer-shelf, whereas in Nielsen Basin, fast-flowing ice was prevalent along all of its grounded length and MSGs indicate ice flow into the trough from the adjacent West Storegg Bank. The location of a former grounding zone can be inferred from GZWs located near the continental shelf break at identical water depths (~390 m) in both troughs (Mackintosh et al., 2011) (Fig. 3). These GZWs also coincide with transitions from fluted substrate (indicative of grounded ice) to populations of keel marks (marking iceberg armadas). Landward of the inferred grounding zones, each trough contains a post-glacial sediment drift. A CHIRP sonar profile shows a 30–50 m thick sediment drift in Iceberg Alley, with multiple, coherent, reflectors overlying a glacially sculpted surface (Mackintosh et al., 2011). Jumbo piston cores through these



sequences provide high-resolution sediment records of the transition from the last glacial to the Holocene, permitting assessment of the timing of deglaciation. Both cores show ice-proximal laminated couplets of diatom ooze at the base of the section indicating marine deposition within a former calving bay reentrant (Leventer et al., 2006). Radiocarbon ages from this section indicate that ice retreat began at or before  $\sim 11.6$  cal ka BP in Iceberg Alley and  $\sim 14$  cal ka BP in Nielsen Basin (calibrated with  $1700 \pm 200$  yr reservoir corrections) (Mackintosh et al., 2011), whilst thick, grounded, ice remained on flanking margins such as West Storegg Bank. The timing of this ice retreat is compatible with the onset of ice-sheet lowering in the adjacent Framnes Mountains (Mackintosh et al., 2011).

The chronologies for the Mac.Robertson Land shelf are consistent with earlier work (Harris and O'Brien, 1998; Sedwick et al., 1998, 2001), that places deglaciation at  $13,390^{14}\text{C}$  yr BP ( $13,468\text{--}14,641$  cal yr BP), based on the initiation of marine sedimentation with the deposition of siliceous muds and oozes. The observation of a bloom of *Chaetoceros* resting spores "associated with the retreat of permanent ice cover" in outer Iceberg Alley at  $\sim 11$  ka BP (Sedwick et al., 2001) may in fact be similar to the calving bay reentrant facies described in Leventer et al. (2006).

#### 4.3. Lambert/Amery drainage basin including Prydz Bay, and the Ingrid Christensen Coast

The Lambert Glacier/Amery Ice Shelf system is one of the largest glacial catchments in Antarctica, draining approximately 16% of the EAIS. Ice flow from as far inland as Dome Argus and Dome Fuji converges into outlet glaciers such as the Lambert, Mellor and Charybdis glaciers that flow through the Prince Charles Mountains in Mac.Robertson Land. These glaciers terminate in the Amery Ice Shelf (Fig. 4), which disgorges icebergs and meltwater into Prydz Bay; a large and roughly rectangular bay between  $60^\circ\text{E}$  and  $80^\circ\text{E}$  (Fig. 4). This embayment is the ice-free part of a major glacial trough eroded by the Lambert-Amery system that extends 1000 km into the continental interior and which reaches up to 2560 m below sea level (Damm, 2007). Exposed rock near the ice domes is rare, with the exception of the Grove Mountains, which outcrop on the eastern flank of the drainage basin.

The Ingrid Christensen Coast (Fig. 4) forms the eastern margin of Prydz Bay, and the glacial history of this region is mostly influenced by local glaciers and the EAIS margin, although isostatic adjustment following ice recession in the Lambert/Amery system has also played a role. Ice-free oases in this part of Antarctica including the Larsemann and Vestfold Hills (Fig. 4) have been the focus of intensive study.

##### 4.3.1. Prince Charles Mountains

The Prince Charles Mountains (Fig. 1) form the eastern margin of the Lambert Glacier and Amery Ice Shelf system. The mountains (culminating in Mt Menzies, 3228 m asl) contain numerous ice-free areas including the Amery Oasis in the northern part of the mountain range. Glacial deposits from the LGM are found on slopes proximal to present-day glaciers and are identifiable as a distinct set of lightly weathered to unweathered sediments, which range from scattered erratics to ice cored moraines and hummocky debris sheets depending on the depositional setting (Bardin, 1982; Mabin, 1991). Above this limit, much older glacial deposits are preserved (Whitehead and McKelvey, 2001; Fink et al., 2006). The LGM deposits show clear evidence for a low angled ice stream in the region occupied by the present day Amery Ice Shelf. Ice thickening in this area was limited to  $\sim 250$  m above present ice shelf height in the vicinity of Loewe Massif (Fig. 1). LGM thickening was greatest ( $\sim 800$  m) at Mt Stinear near the modern-day grounding zone

(Mabin, 1991; White et al., 2011b) (Fig. 1). This thickening diminished inland away from the grounding zone, reaching  $\sim 160$  m at Mt Ruker (Fig. 1), and zero by the present day  $\sim 2000$  m ice surface contour adjacent to the outer nunataks in the Prince Charles Mountains (White et al., 2011b).

Like other inland, mountainous regions in Antarctica, exposure dating in the Prince Charles Mountains is complicated by the cold-based nature of the ice that advanced over the nunataks during the LGM (White and Hermichen, 2007; White et al., 2011b). Thus, our Supplementary data table includes ages that are within 1–2 ka of the youngest exposure age at any one elevation relative to the ice sheet margin at each site. This includes all samples measured by White et al. (2011b) at Loewe Massif, and approximately half those at Mt Stinear and Mt Ruker. The older, excluded population of samples includes a subset with divergent  $^{10}\text{Be}/^{26}\text{Al}$  ages, and thus clearly contain inherited cosmogenic isotopes.

Ice retreat began as early as 18 ka ago at Loewe Massif (Fig. 1), where TCN age data provide a clear stratigraphic sequence and are correlated with sediment records of retreat of ice from Lake Terasovje (Wagner et al., 2004). Ice reached near to the modern ice margin at  $\sim 12$  ka ago at Loewe Massif, and near the modern grounding zone at Mt Stinear around 9 ka ago (White et al., 2011b).

##### 4.3.2. Prydz Bay

The bathymetry of Prydz Bay is broadly similar to the rest of the Antarctic shelf, with an inwardly deepening continental shelf approaching depths of 1000 m in the southwestern corner of the bay and  $\sim 700$  m in the Amery Depression along the front of the Amery Ice Shelf (Fig. 4). The Amery Depression shoals gently to outer shelf banks (Four Ladies Bank) around 100–200 m deep, while the shelf break is at around 400–500 m in the Prydz Channel, a 100 km wide cross-shelf trough typical of glaciated margins cut by an ice stream (Fig. 4) (O'Brien and Leitchenkov, 1997). The southeastern side of the bay features a series of troughs and saddles collectively named the Svenner Channel. Prydz Bay receives ice from large glaciers that flow into the Amery Ice Shelf as well as from the southeastern side of Prydz Bay, the Ingrid Christensen Coast. The Ingrid Christensen Coast features some smaller outlet glaciers which flow around ice-free areas such as the Vestfold and Larsemann Hills. Svenner Channel (Fig. 4) is a series of over-deepened topographic basins where these glaciers extended and joined the main Amery Ice Shelf flow during major glaciations.

The sea floor at Amery Depression and Prydz Channel (Fig. 4) contains abundant MSGs (O'Brien and Leitchenkov, 1997) that terminate at their seaward ends by GZWs running obliquely across Prydz Channel (East Prydz Channel-1) and the Lambert Deep, a topographic basin 1100 m deep in the southwestern corner of Prydz Bay (Fig. 4) (O'Brien et al., 1999). The GZWs on the western side of Prydz Channel (West Prydz Channel 1–3) run along the border of the Channel and Fram Bank parallel to the Channel axis. GZWs are difficult to identify in water shallower than 500 m because of iceberg scouring (O'Brien and Leitchenkov, 1997).

The GZW arranged along Prydz Channel are low asymmetric ridges. However, where the West Prydz Channel-1 wedge becomes the downstream end of the Lambert Deep (Fig. 4), it reaches 300 m in height above the floor of Prydz Channel. This wedge contains complex internal stratigraphy comprising eroded lower units and upper offlapping sediment wedges indicating repeated progradation of sediment delivered by the ice stream flowing in Lambert Deep. Two smaller GZWs were deposited by retreat of the Lambert Deep glacier (Fig. 4).

Cores have been taken across Prydz Bay, including beneath the Amery Ice Shelf (Hemer and Harris, 2003; Hemer et al., 2007), with an array clustered around the East Prydz Channel-1 GZW on the mid-shelf region (Fig. 4) (O'Brien and Leitchenkov, 1997; Domack

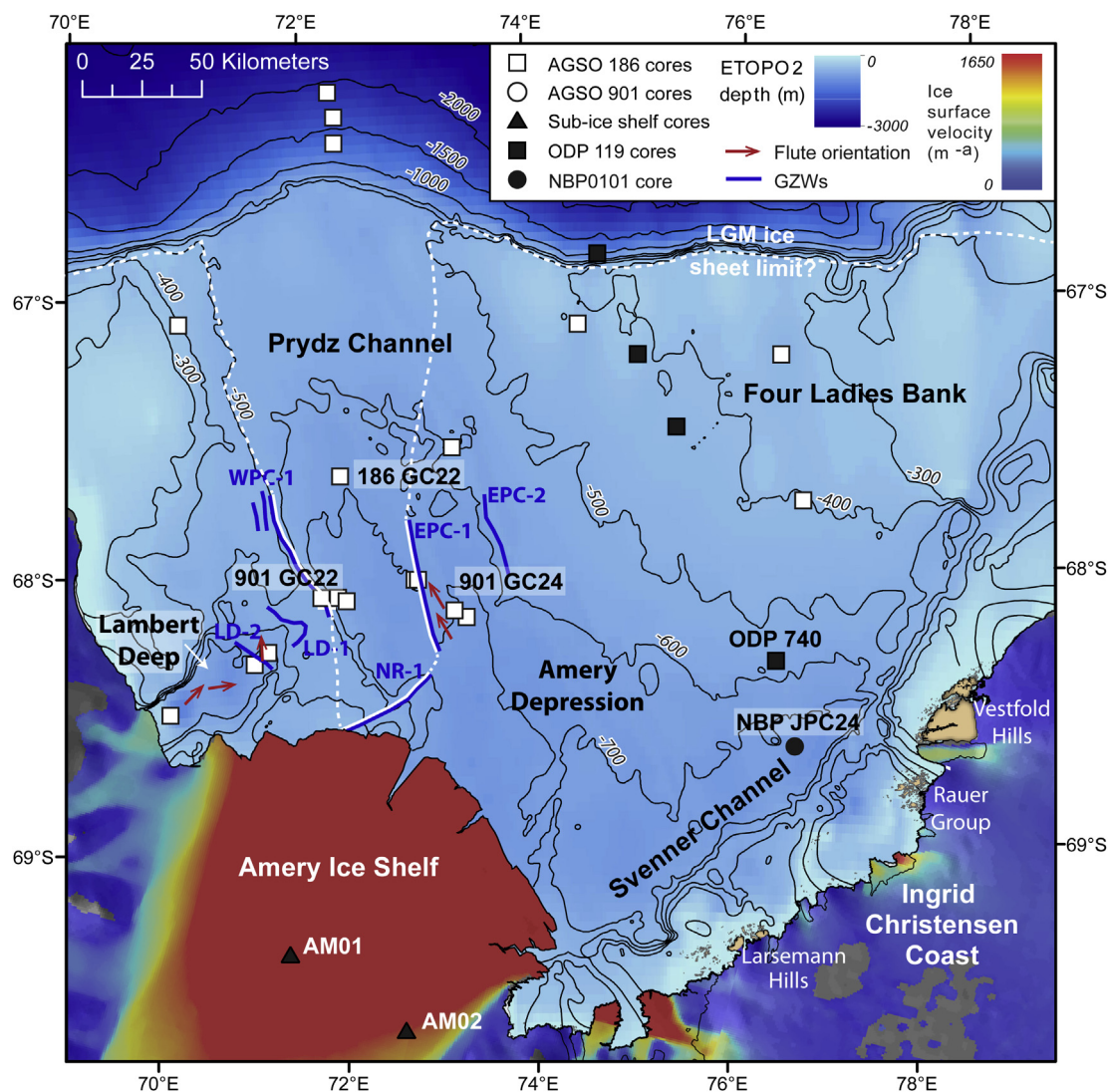


**Fig. 4.** Map of the Prydz Bay region including the Amery Ice Shelf, Prydz Channel, Svenner Channel, Four Ladies Bank, Larsemann Hills, Rauer Group and Vestfold Hills. Bathymetry and the location of sediment cores are also shown. East Prydz Channel (EPC), West Prydz Channel (WPC), Lambert Deep (LD) and Nella Rim (NR) grounding zone wedges are marked. The LGM grounding zone position is constrained by these grounding zone wedges, and is inferred in other locations. Ice-free areas are marked in brown.

et al., 1998). Cores on the upstream flank of this GZW show a succession comprising a lower olive grey diamict overlain by diatom-bearing mud and diatom oozes (Domack et al., 1998). These facies represent subglacial deposition followed by ice retreat and marine deposition. In some cores (e.g. AGSO186/GC24), the transition from subglacial diamict includes a bed of granulated sandy mud to diamict formed by deposition from compacted basal debris melting from the base of an ice shelf (Domack et al., 1998) and beds of silty clay representing sedimentation beneath the ice shelf before the input of open marine diatomaceous material started. Dating of the AIOM from diatom ooze just above the transition from diamict gives an age of  $12,680 \pm 110$   $^{14}\text{C}$  yr BP (Domack et al., 1998) (12,899–13,580 cal yr BP).

Integrated Ocean Drilling Programme (IODP) Site 740 (Leg 119) intersected a thick Holocene section in Svenner Channel near the southeast side of Prydz Bay (Domack et al., 1991). These sediments are mostly siliceous muddy ooze and clay overlying glaciomarine clay. Their position in Svenner Channel (Fig. 4) means that open water sedimentation could not have begun here until grounded ice had retreated from Four Ladies Bank. The AIOM  $^{14}\text{C}$  date from the siliceous ooze just above the boundary with glaciomarine clay

presented by Domack et al. (1991) is  $11,140 \pm 75$   $^{14}\text{C}$  yr BP (10,894–11,747 cal yr BP). Nearby, also in the Svenner Channel (Fig. 4), cruise NBP0101 recovered a 24 m jumbo piston core (NBP0101 JPC24) that penetrated glacial sediments (Leventer et al., 2006). The “calving bay reentrant facies” of rhythmically laminated sediment couplets is represented by a 22 cm thick section that overlies glacially deposited greenish grey sandy and silty clay, with sand- to gravel-sized ice-rafted grains and granule-rich clay. Core chronology was based on carbonate-based ( $n = 5$ ) and AIOM ( $n = 2$ )  $^{14}\text{C}$  dates. Radiocarbon ages were calibrated using a reservoir age of  $1280 \pm 200$  years, based on a kasten core surface age from the same site. The timing for the initiation of deglaciation occurs at  $\sim 11,000$  cal yr BP, based on extrapolation of a best-fit line on the carbonate-based dates (Leventer et al., 2006; Barbara et al., 2010).

Hemer et al. (2007) described a set of short cores taken beneath the Amery Ice Shelf through hot water drill holes (Fig. 4). They show a diatom rich interval representing advection of pelagic material into the sub ice shelf cavity overlying siliciclastic rich sediments. The siliciclastics comprise a lower pebbly sandy mud unit overlain in places by bedded and cross-bedded sands and silts. Hemer et al. (2007) reported an age for the base of the siliceous muddy ooze

layer of  $13,529 \pm 50$   $^{14}\text{C}$  yr BP (13,800–14,652 cal yr BP). If this age is calibrated and corrected using the surface age, it becomes 10,768–11,141 cal yr BP (Supplementary data table). This latter age is more consistent with the age for onset of open water sedimentation in Prydz Channel discussed above. The underlying silts and sands represent a period of intense current activity caused by thermohaline circulation enhanced by tidal pumping in the narrow cavity soon after ice lift off (O'Brien et al., 1999; Hemer et al., 2007). Dates from these units are as old as 28,250  $^{14}\text{C}$  yr BP but their dark colouration suggests contamination by recycled carbon, such as coal-bearing material from Lambert Graben sediments (Hemer et al., 2007).

In summary, evidence from Prydz Bay indicates that LGM ice advanced to the position of the GZWs in the mid shelf around Prydz Channel and further towards the shelf edge on Four Ladies Bank (Fig. 4). Coring seaward of the GZW (Domack et al., 1998) and drilling on the continental slope suggest that glacial ice has not been grounded to the shelf edge in Prydz Channel since the mid-Pleistocene (O'Brien et al., 2007). Estimating the timing of glacial retreat from the mid-shelf using AIOM is difficult because of reworked carbon in the sediment, but existing data suggests that the onset of open water sedimentation took place at  $\sim 13$  cal ka BP at the East Prydz Channel-1 grounding zone (Domack et al., 1998) and spread to sites beneath the present Amery Ice Shelf by  $\sim 11$  cal ka BP (Hemer et al., 2007). Open water sedimentation also reached the Svenner Channel later at  $\sim 11$  cal ka BP (Domack et al., 1991; Leventer et al., 2006; Barbara et al., 2010), suggesting that grounded ice may have persisted over Four Ladies Bank while the grounding zone of the Amery Ice Shelf retreated along Prydz Channel.

#### 4.3.3. Grove Mountains

The Grove Mountains are an isolated group of nunataks 500 km south of Vestfold Hills (Fig. 1), hundreds of kilometres east of Lambert Glacier. The ice sheet elevation is around 2000 m asl, and the ice is slow flowing. Geomorphic evidence of former ice cover includes large-scale erosional landforms and glacially transported boulders and sediments, but TCN exposure dating of both bedrock and glacially transported material has found no evidence for a greater ice thickness at the LGM relative to today. Modelling of measured  $^{10}\text{Be}$  and  $^{26}\text{Al}$  concentrations in bedrock samples suggests that the surface elevation of the EAIS at this location was likely lower at the LGM than today (Lilly et al., 2010). Ten erratic samples measured in an elevational transect ranging from 1 to 90 m above present-day ice surface range in age ( $^{10}\text{Be}$  minimum exposure age) from 50 to 900 ka ago, suggesting that the ice sheet surface reached an elevation at or below present elevation long before the LGM at  $\sim 50$  ka ago (Lilly et al., 2010).

#### 4.3.4. Larsemann Hills

The Larsemann Hills are a 50 km<sup>2</sup> coastal oasis of low-lying peninsulas and islands on the Ingrid Christensen Coast (Fig. 4), west of Dalk Glacier. Hilltops are typically glacially rounded, and more than 150 freshwater lakes and ponds occupy depressions in the outer islands and the two major peninsulas, Broknes and Stornes (Hodgson et al., 2006b). Erratics are rare, and the bedrock highly weathered (Kiernan et al., 2007). Bedded glaciofluvial sands on southwestern Broknes have been OSL-dated to the LGM (Hodgson et al., 2001), but evidence from lake sediment cores shows that at least some parts of Broknes remained ice free through the LGM (Hodgson et al., 2005). In contrast, Stornes was covered by an expanded version of the small local ice dome that presently occupies the southern portion of the peninsula (Burgess et al., 1994; Hodgson et al., 2001; Kiernan et al., 2007). OSL,  $^{14}\text{C}$ , and TCN ages from Broknes suggest an extensive ice-free period, while those near the ice sheet margin at Broknes and on Stornes indicate progressive

removal of ice and snow, and retreat of the ice sheet in this region of  $\sim 5$  km during the Holocene (Hodgson et al., 2001). Emergent shorelines up to 8 m asl reflect increases in regional ice loading during the LGM (Verleyen et al., 2005).

#### 4.3.5. Vestfold Hills and Rauer Group

The Vestfold Hills form one of the largest ice-free zones on the East Antarctic coast with an area of  $\sim 410$  km<sup>2</sup> (Fig. 4). They are separated from the Larsemann Hills by Sørsdal Glacier and the Rauer Islands. Its coastline is a complex of small rocky islands and fjords with water depths reaching up to 160 m. Islands and hills on the mainland reach elevations of up to 60 m in the coastal zone, and rising to 159 m inland near the ice sheet margin.

The Vestfold Hills form a low elevation plateau surrounded by Sørsdal Glacier to the south, the ice sheet to the east, and the ocean to the north and west. The Sørsdal Glacier trough is at least 750 m deep and the sea floor drops to depths of 300–700 m in the Svenner Channels to the west (O'Brien and Leitchenkov, 1997).

Glacial sediments are found across the Vestfold Hills, but they are thickest in the west of the Hills where marine salts enhance weathering of bedrock and erratics (Gore et al., 1996, 2003). Glacial sediments there are commonly fossiliferous, as advancing ice eroded and deposited debris from the fjords and salt lakes (Gore et al., 1994). Marine sediments are found along ENE–WSW trending valleys in the form of fossiliferous sands deposited around glacially-transported boulders. In places diatom-bearing sands drape low relief plains within the valleys. Sections through these sediments are exposed in benches around some lakes (Pickard et al., 1988). Isostatic rebound has transformed some former fjords into isolation basins, and ultimately lakes. Some lakes have then become fresh through flushing by snow melt or stream flow, whereas others have continued to evaporate to become saline to hypersaline, and some now have water levels tens of metres below sea level.

$^{14}\text{C}$  dating of organic remains in emergent shorelines and isolation basins to  $<10$  m asl were used in conjunction with a simplified ice sheet model to reconstruct a regional loss of 600–700 m in ice thickness since the LGM (Zwartz et al., 1998). However, this regional ice sheet reconstruction does not preclude an absence of ice on Vestfold Hills at the LGM. Erratics scattered across Vestfold Hills and the adjacent Rauer Group (White et al., 2009) indicate extensive glaciation some time in the past, but the timing of deglaciation remains unclear. Extensive radiocarbon sampling from lakes, uplifted former marine sediments and remains of penguin colonies indicate Vestfold Hills has been ice free for at least the past  $8865 \pm 10$   $^{14}\text{C}$  yr BP (Huang et al., 2009) (8189–8656 cal yr BP) near the coast,  $8260 \pm 110$   $^{14}\text{C}$  yr BP (Pickard and Seppelt, 1984) (7556–8134 cal yr BP) at Watts Lake, and  $18,810 \pm 440$   $^{14}\text{C}$  yr BP (21,408–23,550 cal yr BP) at Lake Abraxas (Gibson et al., 2009). TCN dating of erratics from the northeast of the Vestfold Hills adjacent to the ice sheet confirm that deglaciation was essentially complete by  $\sim 11$  ka ago (Fabel et al., 1997). However, the extent of ice coverage and the timing of its removal has been long debated, and recent work on lake sediments suggests that the northwestern part of the Vestfold Hills may have been ice free during the LGM (Gibson et al., 2009).

The timing of the last major period of ice occupation in the Rauer Group (Fig. 4) remains poorly constrained. Although the ice sheet likely occupied the entirety of the islands during the final half of the last glacial cycle (White et al., 2009),  $^{14}\text{C}$  ages from a marine sediment core indicate ice-free conditions existed at  $\sim 30$  ka BP (Berg et al., 2009). This was followed by a period of glaciation (Berg et al., 2009, 2010a). Ice retreated from the middle of the archipelago by  $12,490 \pm 80$   $^{14}\text{C}$  yr BP (Berg et al., 2010a) (12,735–13,306 cal yr BP), and reached the ice margin by  $5000 \pm 35$   $^{14}\text{C}$  yr BP (Berg et al., 2010b) (3852–4424 cal yr BP), although the latter age is a minimum constraint (Berg et al., 2010a).



#### 4.4. Wilkes Land

Wilkes Land is vast, extending from  $\sim 100$  to  $140^\circ$  E (Fig. 1). Ice-free regions are relatively scarce, and geological constraints are only available from the Bunger Hills (Figs. 1 and 5) and Windmill Islands (Figs. 1 and 6). Very limited data are available from the continental shelf regions. Only Vincennes Bay (Fig. 6) adjacent to the Windmill Islands has been studied.

##### 4.4.1. Bunger Hills

Bunger Hills are a  $950 \text{ km}^2$  ice-free area that lies between the EAIS to the east, Apfel Glacier to the south and Shackleton Ice Shelf to the west and north (Fig. 5). The physiography of Bunger Hills is similar to Vestfold Hills, in that both have an outlet glacier to the south and ice sheet to the east. They have similar land areas, topographic relief, orientation of marine inlets, freshwater, saline and hypersaline lakes, sediments and height of emergent shorelines at  $\sim 10 \text{ m asl}$  (Colhoun and Adamson, 1989; Colhoun et al., 1992). Like Vestfold Hills, the regional glaciation of Bunger Hills came from the southeast and the fringing glacier to the south has had a minor northwards expansion (and retreat) since the retreat of the ice sheet. Where they differ is in other aspects of their glaciology, with Bunger Hills being delimited to the west and north by a floating ice shelf whereas Vestfold Hills has open sea. More importantly though, the two areas have differing glacial histories with the Vestfold Hills probably becoming ice free at the start of the Holocene (but see Gibson et al., 2009), whereas the inner, higher parts of Bunger Hills deglaciated prior to the LGM.

Two dating methods have been used to construct this deglaciation chronology – OSL dating of glaciofluvial and glaciolacustrine sands (Gore et al., 2001), and  $^{14}\text{C}$  on marine shells (Adamson and Colhoun, 1992), lake sediments (Melles et al., 1994; Roberts et al., 2000; Kulbe et al., 2001; Verkulich et al., 2002) and mumiyo deposits. The OSL age estimates (Gore et al., 2001) are consistent with earliest exposure of the hilltops from the thinning ice sheet at around 40–30 ka ago (Fig. 5). Slow moving or cold-based ice continued to encroach upon the oasis from all sides at this time. Following the LGM, further thinning and recession of ice occurred, allowing the formation of large glacial lakes (Colhoun and Adamson, 1989) against topographic high points from 20 ka ago (Gore et al., 2001). The large, prominent glacial lake shorelines that line many valley walls in the western part of the oasis are dated to 15–10 ka ago, consistent with a  $13,600 \pm 140 \text{ yr BP } ^{14}\text{C}$  ( $13,825 - 15,020 \text{ cal yr BP}$ ) age from a macrofossil within lacustrine sands (Gore et al., 2001) (Fig. 5). The oasis attained its present size by the start of the Holocene, allowing the glacial lakes to drain and their shorelines to be stranded up to tens of metres above modern sea level.  $^{14}\text{C}$  dating of lake sediments and mumiyo deposits do not reflect this pre-LGM exposure of the oasis from the ice, most likely due to the blanketing effects of permanent snow and superimposed ice which precluded most biological activity in the oasis prior to the Holocene (Gore, 1997).

##### 4.4.2. Windmill Islands and adjacent continental shelf

The Windmill Islands form an ice-free oasis ( $75 \text{ km}^2$ ) that extends perpendicularly 15 km offshore from the Law Dome ice margin and parallel to the Vanderford Glacier axis (Fig. 6).

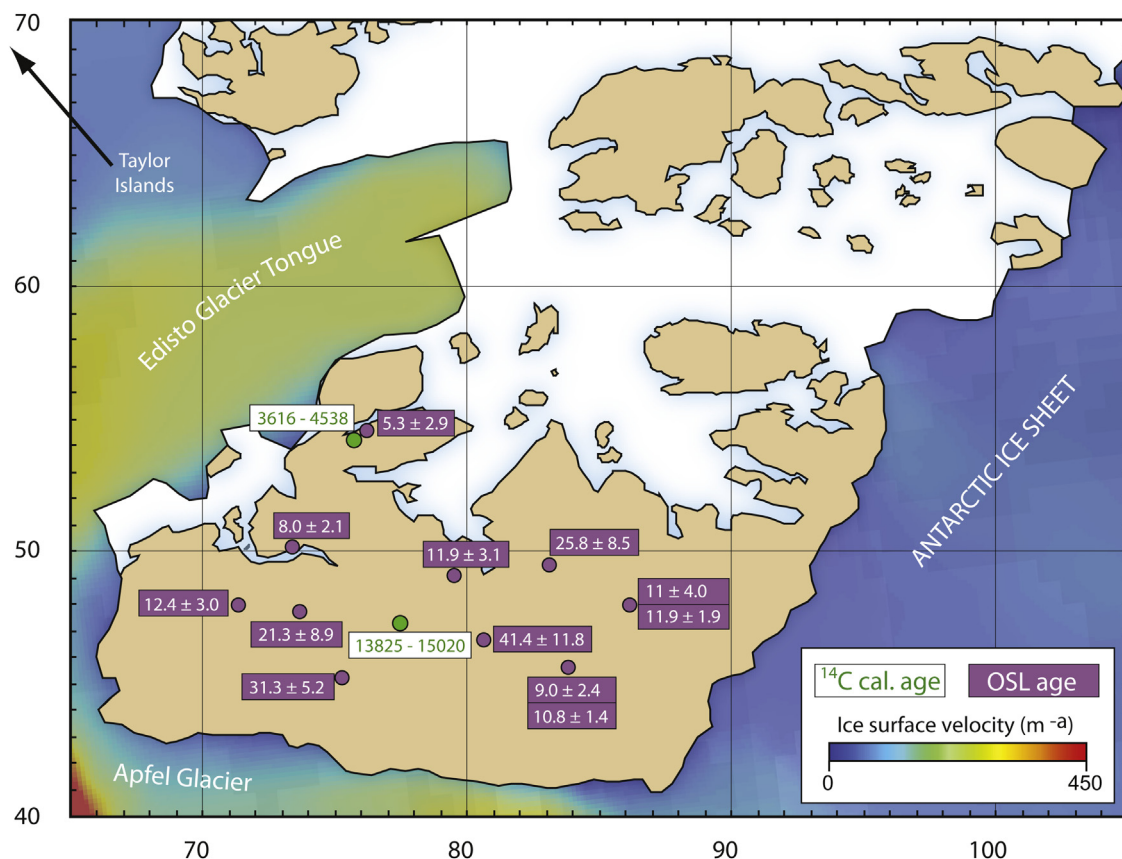


**Fig. 5.** Map of Bunger Hills, Wilkes Land, one of the largest ice-free oases in East Antarctica. The surrounding East Antarctic Ice Sheet, Apfel Glacier and the floating Edisto Glacier Tongue are shown, including flow velocities (Rignot et al., 2011). Bunger Hills preserves pre-LGM fluvial and lacustrine sediments dated by luminescence, indicating that the central part of the oasis remained ice free at the height of the last glaciation.

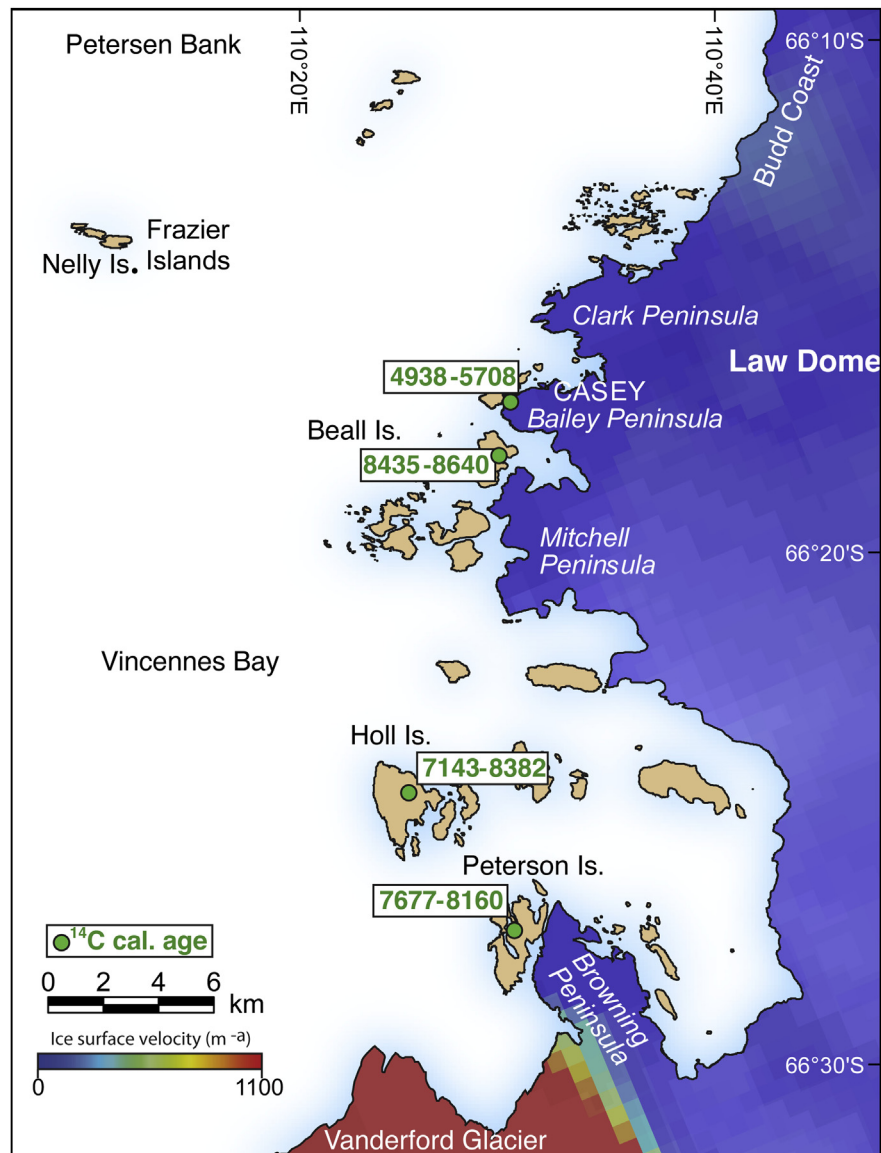


**Fig. 6.** Map of Windmill Islands, Wilkes Land, showing the distribution of islands, peninsulas and the adjacent ice including fast-moving Vanderford Glacier and slow-flowing Law Dome (Rignot et al., 2011). The timing of deglaciation onset is not known, but  $^{14}\text{C}$  ages from Holl, Peterson and Beall Islands, as well as the Bailey Peninsula, indicate that ice retreat was mostly complete by  $\sim 8$  ka BP.

Vincennes Trough, adjacent to these islands, extends to 2000 m water depth on the inner shelf.

The Windmill Islands show morphological and sedimentological evidence for previous glacial over-riding and geologically recent partial deglaciation. Ubiquitous weak to moderate bedrock weathering, glacial erratics and striae together with a suite of raised beaches to 32 m elevation above modern mean sea level are observed across the Windmill Islands (Goodwin, 1993). Rare red sandstone erratics found below 30 m elevation and particularly on the outer islands (Nelly Island, Frazier Island Group and Browning Peninsula in the southern Windmill Islands, Fig. 6) attest to former glacial expansion of the Vanderford Glacier draining the ice along the Budd Coast. Several studies have attempted to produce a minimum age deglacial history from the LGM for the Windmill Islands (Goodwin, 1993, 1996; Kirkup et al., 2002; Cremer et al., 2003; Hodgson et al., 2003), whilst a maximum age for ice retreat was constrained by the late Holocene chronology for renewed ice sheet advance (Goodwin, 1993, 1998, 1996).

Goodwin (1993) reported a minimum age for ice margin retreat at  $8160 \pm 300$   $^{14}\text{C}$  yr BP (7143–8382 cal yr BP) from radiocarbon ages on biogenic marine sediments at the base of sedimentation in Holl Pond on Holl Island in the southern Windmill Islands (Fig. 6), and  $5930 \pm 120$   $^{14}\text{C}$  yr BP (4938–5708 cal yr BP) at Bailey Peninsula in the northern Windmill Islands (Fig. 6), near the upper marine limit. Roberts et al. (2004) and Hodgson et al. (2006a) reported a basal date for Beall Lake on Beall Island of  $7840 \pm 40$   $^{14}\text{C}$  yr BP (8435–8640 cal yr BP).

Kirkup et al. (2002) analysed an organic-rich marine deposit (sapropel) overlying till, and a sapropel sequence from a sediment core obtained from an epishelf lake on Peterson Island in the southern Windmill Islands. They concluded that the area was glaciated after  $26,130 \pm 950$   $^{14}\text{C}$  yr BP (27,788–31,205 cal yr BP), with deglaciation commencing before  $8360 \pm 60$   $^{14}\text{C}$  yrs BP (7677–8160 cal yr BP), although an extrapolation based on the sediment accumulation rate indicates probable deglaciation earlier at  $\sim 10.7$  ka BP. Since the Peterson Island site lies on the eastern boundary of the Vanderford Glacier/Vincennes Bay trough (Fig. 6),

the minimum age for deglaciation most probably reflects the retreat of the Vanderford Glacier. [Cremer et al. \(2003\)](#) and [Hodgson et al. \(2003\)](#) extended this work from the analysis of two epishelf sediment cores from Peterson Inlet and Browning Bay in the south Windmill Islands and concluded that sapropel sedimentation commenced at  $\sim 10.5$  cal ka BP, following deglaciation. In summary, the onshore sedimentary evidence indicates that the south Windmill Islands were deglaciated by  $\sim 10.5$  cal ka BP and the north Windmill Islands were deglaciated by  $\sim 8.5$  (Beall Island) to  $\sim 5.5$  cal ka BP (Bailey Peninsula). This small difference in timing may reflect the differential in the earlier Vanderford Glacier retreat compared to the Law Dome ice margin retreat, although this deglacial record remains under-constrained by replicate sites.

[Goodwin and Zweck \(2000\)](#) used a glacio-isostatic model to investigate the deglacial history of Law Dome. Using available  $^{14}\text{C}$  ages and the observed 32 m isostatic marine limit, they modelled an LGM ice sheet with a thickness ranging from 770 to 1000 m grounded over the Windmill Islands that extended 40–65 km offshore over the Petersen Bank.

The offshore evidence for LGM glaciation in this region is scant. Several seabed sediment cores were obtained from Vincennes Bay showing a dominant terrigenous glaciomarine sediment deposition throughout the late Quaternary in the overdeepened inner shelf trough ([Harris et al., 1997](#)). Further offshore sediment cores from the Petersen Bank in 500–600 m of water contain a diamict, separated by thin Ice Rafted Debris layers (IRD) that indicate grounding of the expanded Vanderford Glacier prior to the Holocene. The radiocarbon dates determined from foraminifera in the overlying silicious mud and ooze yielded ages older than 20,000  $^{14}\text{C}$  yr BP, and are most likely incorrect. Hence, the offshore history of the post LGM retreat in Vincennes Bay remains unconstrained.

#### 4.5. George V Land – Terre Adélie shelf

This region of the EAIS occurs between Wilkes Land and the Transantarctic Mountains ([Fig. 1](#)), and includes major outlets including the Mertz and Ninnis Glaciers. No geological constraints are available from onshore in this region, but offshore troughs have been relatively well studied.

The deglacial history in this region is mostly constrained by evidence from the Mertz Trough, George V, and Adélie Basins, three adjacent  $>1000$  m deep, glacially-scoured troughs separated by the 200-m deep Mertz Bank and Adélie Bank ([Fig. 7](#)). Bathymetric surveys, and sedimentary studies of diamicts within these troughs indicate that outlet glaciers along this coastline extended to the shelf edge, most likely during the LGM, with the shallow shelf banks heavily reworked by iceberg scour ([Domack, 1982](#); [Escutia et al., 2003](#); [Presti et al., 2003](#); [Leventer et al., 2006](#); [McMullen et al., 2006](#)). MSGLs indicate that ice flow in the George V Basin and Mertz Trough during the LGM resulted from interplay between the Mertz and Ninnis glaciers, while the Adélie Basin was fed by ice derived from both the Zélée and Astrolabe Glaciers ([Fig. 7](#)) ([Eittrheim et al., 1995](#); [Beaman and Harris, 2003](#); [McMullen et al., 2006](#); [Beaman et al., 2011](#)). Two linear ridges on the Mertz Bank are aligned parallel to the adjacent trough sand and are interpreted as representing LGM lateral moraines marking the divide between streaming ice in the troughs and less mobile grounded ice on the shelf banks ([Eittrheim et al., 1995](#)). However, similar features in the Ross Sea are interpreted as being deposited during retreat of grounded bank ice in the absence of grounded ice in the troughs, suggesting that grounded ice remained on the Mertz Banks after retreat occurred in the trough ([Shipp et al., 1999](#)). Two transverse ridges, interpreted as GZWs, also occur in the Mertz Trough and appear to be extensions of the bank ridges ([Eittrheim et al., 1995](#);

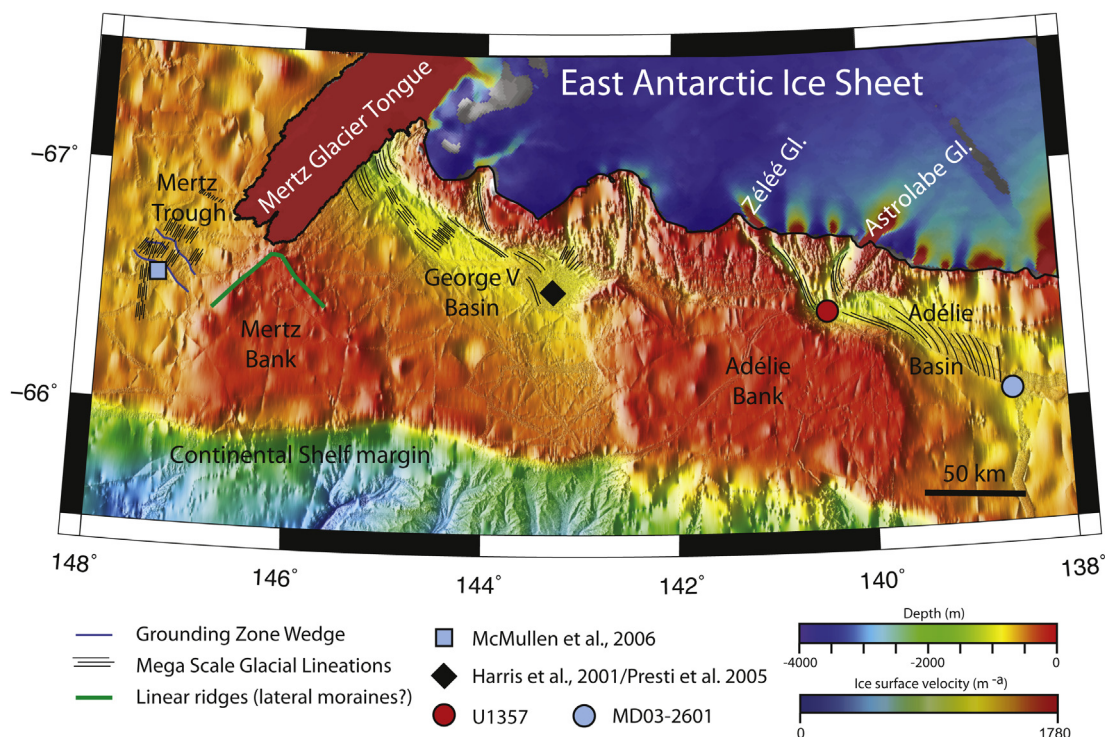


**Fig. 7.** Map of George V Land/Terre Adélie Shelf, showing the major glaciers, basins and troughs, as well as the location of sediment cores. Shelf landforms including grounding zone wedges and mega scale glacial lineations are also shown. The LGM grounding zone occurred seaward of the inner shelf, but its exact location is not known. Shelf bathymetry is derived from [Beaman et al. \(2011\)](#) and ice velocity from [Rignot et al. \(2011\)](#).



McMullen et al., 2006), although MSGs present on the outer shelf to the north of these ridges suggest they were formed during the glacial retreat phase (McMullen et al., 2006) (Fig. 7).

A suite of kasten cores from the Mertz Trough (Fig. 7) collectively recovered a stratigraphic succession of massive diamict, overlain by laminated diatom ooze passing up into a ~50 cm of bioturbated clay rich, diatom bearing mud at the surface (McMullen et al., 2006). The massive diamict was sampled from on top of a GZW and therefore represents subglacial deposition at the grounding zone during a pause in ice retreat in the mid-shelf region. The diatom ooze represents pelagic sedimentation after the ice retreated, whereas the overlying diatom-bearing muds with higher terrigenous input is interpreted to correspond with cooling at the onset of the Neoglacial in the late Holocene (McMullen et al., 2006). Radiocarbon dates from these cores were mostly derived from AIOM, however, some calcareous fossils were dated. The oldest carbonate age from these cores is  $5575 \pm 35$   $^{14}\text{C}$  yr BP. As this overlies a younger carbonate date and because the transition from subglacial to open water facies was not recovered in this core, the age of glacial retreat is not constrained by this age. The only core (KC-2) to recover the contact between diamict and diatom ooze gives an age of  $6240 \pm 50$  yr  $^{14}\text{C}$  BP (~15 cm above the contact McMullen et al., 2006). The condensed (i.e. 65 cm thick) and bioturbated nature of the overlying diatom ooze, in combination with the old surface age based on AIOM in this core precludes a reliable core-top correction. For these reasons, we do not provide calibrated ages for this site.

In the George V Basin (Fig. 7), sediment focussing has allowed for thick pelagic diatom oozes to be deposited throughout the Holocene. Ten piston cores from the George V Basin exhibit a different stratigraphy to that in the Mertz Trough (Harris et al., 2001; Presti et al., 2003, 2005). The George V Basin acted as a sediment trap but bottom water formation has reworked sediment into a mounded drift deposit (Harris et al., 2001). Cores display an upper interval of diatom ooze and diatom bearing clay overlying diamict in the bottom of the cores. Tying the cores to shallow depth seismic lines indicates that the diamict is within the well-stratified sediment undisturbed by glacial deformation. This has been interpreted as a sub-ice shelf or subglacial lake deposit formed during the ice advance which deformed the sea floor at depths shallower than 775 m (Presti et al., 2003, 2005). Retreat of glacial ice was accompanied by deposition of oozes and diatom rich mud through most of the Holocene. IRD-rich muddy sands are found at the top of the cores, representing a change to modern cooler conditions.

Dates from just above the transition from sub-ice shelf or subglacial lake sediment to open water conditions give ages of 11,148, 15,469 and 16,807  $^{14}\text{C}$  yr BP (11,004–11,732, 16,889–17,628 and 18,523–18,925 cal yr BP). The oldest of these dates is clearly compromised by recycled organic matter, as the down-core ages imply an order of magnitude of increase in the sedimentation rates at the base of the siliceous muds and oozes units (Harris et al., 2001; Presti et al., 2003, 2005). The diamict layer produced dates as young as  $19080 \pm 110$   $^{14}\text{C}$  yr BP (20,765–21,529 cal yr BP), loosely bracketing the retreat of the George V Basin ice to around 11.3–21.2 cal ka BP, although due to reworking of old carbon we do not consider these ages to be a strong constraint. Additionally, the presence of reworked organic material at this location (Domack et al., 1999; Harris et al., 2001; Harris and Beaman, 2003) results in surface ages that are older than the average reservoir correction for Antarctica. For example, Harris and Beaman (2003) present  $^{14}\text{C}$  dates from 23 surface sediment samples, with a mean  $^{14}\text{C}$  age of  $2583 \pm 443$  yr BP. Domack et al. (1989) suggest reservoir corrections as high as 5500 years for this part of the Antarctic margin, and therefore the 1300 year correction we mostly apply in this review is conservative and the true “corrected” age is potentially much younger. Thus, there is not a reliable estimate for the age of

deglaciation of the George V Basin. The presence of clear GZWs means that additional, deeper sampling of sediment in this trough would be valuable.

The Adélie Basin (Fig. 7) currently offers the best opportunity to constrain the timing of deglaciation in this region. A 40 m long piston core (MD03-2601) indicates that diatom oozes have been deposited in this basin since at least  $10,855 \pm 45$   $^{14}\text{C}$  yr BP (10,604–11,151 cal yr BP), although this core did not penetrate into diamict or glacial retreat facies (Crosta et al., 2007; Denis et al., 2009). More recently, IODP site U1357 was triple-cored in the Adélie Basin on the inner continental shelf, approximately 35 km from the modern-day grounding zone of the Astrolabe Glacier (Fig. 7). It consists of 185.6 m of diatom ooze and mud-bearing diatom ooze overlying massive diamict, making it the highest resolution marine record of the post-LGM sedimentation from the Antarctic (Escutia et al., 2011). The massive sandy clast-rich diamict at the base of hole U1357A is over-consolidated and contains clasts of various lithologies including granite, metasediment and quartzite, consistent with subglacial transport from Adélie Land (Goode and Fanning, 2010). Overlying the diamict is a 15-m-thick interval of clay-bearing to clay-rich diatom ooze, with well-defined repeating couplets of diatom ooze and mudstone-bearing diatom ooze ~1–4 cm thick. This depositional environment persisted for at least 375 years if these laminae represent annual varves, as observed in the Neoglacial section of a nearby core (Maddison et al., 2012). Smear slides indicate that the terrigenous content of diatom oozes in U1357 averages 30%, with  $^{14}\text{C}$  dates on bulk sediment in this interval ranging between ~13 and 40 cal ka BP and likely contaminated by old reworked carbon.

The 15 m-thick terrigenous-bearing interval in U1357 passes sharply up into 170 m of diatom ooze, with well-defined light to dark laminae, interpreted as representing seasonal variations in diatom deposition (Escutia et al., 2011). Smear slide observations indicates that this ooze is remarkably pure, with diatom abundances averaging 90%, and Total Organic Carbon concentrations ranging between 1 and 2% (Escutia et al., 2011). This unit is interpreted as being deposited in seasonally open water conditions, following ice retreat at this site. Site U1357 was triple cored, and a total of 141 AMS  $^{14}\text{C}$  dates on bulk sediment have been collected from holes A, B, and C. Ages which help to constrain the timing of deglaciation are included in the Supplementary data table. A marine radiocarbon correction of  $1235 \pm 200$  years was used to calibrate these dates. We have previously used a 1200 year total reservoir age correction for Adélie Basin carbonate samples (Maddison et al., 2012). This is only slightly higher than a recent estimate of  $1144 \pm 120$  years for the Southern Ocean reservoir age during the Holocene (Hall et al., 2010), and overlaps within error with the marine reservoir correction applied elsewhere in this paper ( $1300 \pm 100$  years; Berkman and Forman, 1996).

More precise estimation of the marine reservoir age at the Adélie Drift IODP coring site is possible because we have a surface sediment sample which yielded a  $^{14}\text{C}$  age of  $1330 \pm 30$  years (uncalibrated, see Supplementary data table). We also observe an average 500 year offset between carbonate shell dates and acid-only treated bulk organic  $^{14}\text{C}$  dates from the upper 50 m of the section. We therefore conclude that there is a background addition of “old” Carbon adding 500 years to the observed  $^{14}\text{C}$  ages prior to calibration using a total reservoir age of  $1235 \pm 200$  years. Most of the dates shown in the Supplementary data table were acid-only (AO) treated. However, we include one acid–base–acid (ABA) date from which we subtract an additional 100 years prior to calibration to account for a consistent offset between AO-treated and ABA treated  $^{14}\text{C}$  ages in the U1357 samples.

Due to the relatively recent collection of the U1357 cores, additional studies are currently being undertaken to further refine

the corrections and calibrations for the dates in this unique core. Based on the calibrated dates presented in the [Supplementary data table](#), sedimentation rates in the uppermost ~170 m-thick diatom ooze unit were ~1.6 cm/yr, implying a relatively high input of autochthonous carbon, with the base of this unit dated at 10,359–11,382 and 10,571–11,756 cal yr BP in holes U1357A and U1357B, respectively. This suggests that the retreat of grounded ice from most of the inner continental shelf to within 35 km of its modern grounding zone in Adélie Basin possibly occurred as early as ~11.5 cal ka BP.

#### 4.6. Ice core evidence and ice sheet models

Several lines of evidence suggest that the interior domes of the EAIS were thinner than present during the LGM, as a result of lower accumulation rates (Jouzel et al., 1989; Siddall et al., 2012). However, the magnitude and spatial distribution of this change in ice sheet thickness is poorly known. Estimates come from two sources, ice cores, which are available at relatively few sites in the ice sheet interior, and ice sheet models, which provide estimates of ice sheet changes for the entire area, but are somewhat unconstrained by field evidence.

Ice core records have long been used to reconstruct the elevation in interior of the EAIS. Two methods are available; using the total gas content of trapped air bubbles within ice cores as a constraint, and 1-dimensional ice flow models tuned to locally-derived estimates of accumulation rate from ice cores. Both methods contain uncertainties that might be larger than the overall signal, and hence must be carefully considered. Nonetheless, estimates of former ice thickness based on this method are consistent with each other, and indicate that the central domes of the ice sheet were >100 m lower than present at the LGM (Table 1) (Fig. 8).

Continental-scale ice sheet model reconstructions do not provide a completely unbiased constraint on former ice sheet thickness. This is because the climate forcing used in most ice sheet models is derived from ice-core observations from the ice sheet interior. Typically this involves making the interior precipitation a function of the  $\delta^{18}\text{O}$  record in ice cores, with a change in total precipitation imposed relative to the present-day pattern. This results in reduced precipitation in the interior of the EAIS at the LGM, and resultant, widespread surface lowering within ice sheet models. The magnitude of ice sheet lowering evident in recent ice sheet modelling studies (Pollard and DeConto, 2009; Mackintosh et al., 2011; Golledge et al., 2012; Whitehouse et al., 2012) compares well to surface elevation changes reconstructed at ice core sites (Table 1), although these constraints cover a small part of the ice sheet interior and some variation between models is evident.

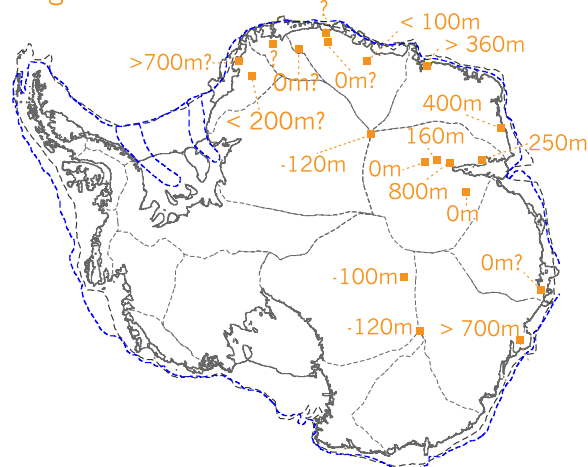
Surface lowering in the EAIS interior is also indicated by moraines (for example along the Amery/Lambert trough (Mabin, 1991; White et al., 2011b)) and dated glacial boulders (e.g. in Framnes Mountains, Mackintosh et al. (2007)), which show that the magnitude of ice sheet thickening observed in coastal regions at the LGM reduced inland. There is also evidence inferred from TCN dating that the LGM ice sheet was thinner than present at the Grove Mountains 500 km inland from the coast (Lilly et al., 2010).

## 5. Discussion and conclusion

### 5.1. How extensive was the EAIS at the LGM?

The EAIS probably advanced to near the continental shelf margin in many places during the LGM. For example, in Mac.Robertson Land, the outermost documented GZWs lie only ~10 km from the shelf break, more than 90 km north of the present-day ice margin (Fig. 3). In this region, LGM ice also grounded within

### a) Change in ice thickness



### b) Timing of deglaciation

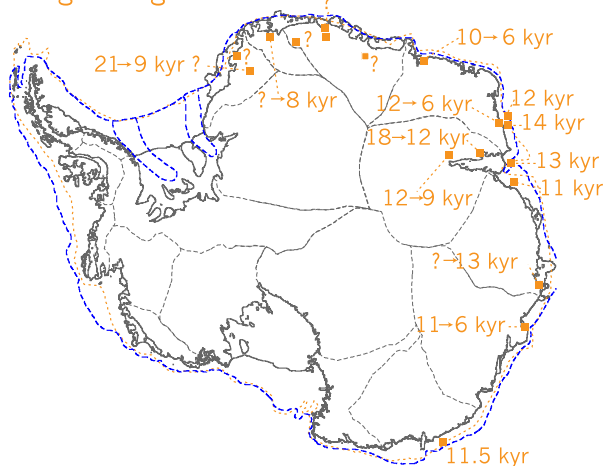


**Fig. 8.** Summary diagram showing (a) approximate changes in ice thickness at the LGM relative to today and (b) the timing of deglaciation at different sites (all data derived from main text, ages rounded to nearest thousand years). Locations are identical to those in Fig. 1. Changes in ice thickness are only shown in locations where chronological control is discussed in the main text. Numbers separated by arrows indicate the onset and cessation of deglaciation. Single numbers on the continental shelf show the timing of onset of marine sedimentation (ice-free conditions). Estimated LGM grounding zone positions are from Anderson et al. (2002) (black line) and Livingstone et al. (2012) (blue line).

troughs on the inner shelf that are more than 1 km deep. In Prydz Bay, the expanded EAIS most likely reached the shelf edge on the Four Ladies Bank (Fig. 4). In contrast, the Lambert/Amery system showed a more restricted advance, either because the ice sheet was unable to expand into deep water within Prydz Channel, or as a consequence of reduced accumulation in the ice sheet interior. In George V Land/Terre Adélie Coast, the inner to mid-shelf was occupied by an expanded ice sheet at the LGM, and geomorphological evidence indicates past ice sheet advance to the shelf edge, most likely during the LGM although chronological constraints are currently lacking from the outer shelf to confirm this. Few data are available from the continental shelf in many regions, including Dronning Maud Land, Enderby Land and much of Wilkes Land (Figs. 1 and 5–7). The LGM extent of the ice sheet in these areas is largely unconstrained.

Evidence for thickening and expansion of the EAIS at the LGM is preserved in several coastal oases and nunatak regions, including Lützow-Holm Bay, Framnes Mountains, Prince Charles Mountains and the Windmill Islands (Fig. 8). Striking evidence of this is found

on the margin of the Lambert Glacier in the Prince Charles Mountains, and these moraine limits represent an important target for ice sheet model simulations. The variation in thickening recorded at each site reflects several factors, including local ice sheet dynamics and distance from the coast. For example, evidence from Framnes Mountains near the present coast indicates a thickening of ~400 m relative to today. In contrast, several inland nunataks in East Antarctica (e.g. Wohlthat Massif, Sør Rondane Mountains, Grove Mountains) show limited or no evidence of LGM ice sheet thickening (Fig. 8), and it is likely that the ice surface decreased in elevation in some of these areas at this time. This inference is supported by ice core evidence and numerical ice sheet models, which indicate that the central domes of the LGM ice sheet were >100 m thinner than present (Table 1).

Evidence from several ice-free oases such as Vestfold and Bunger Hills mostly record changes in local ice sheet extent and changes in the configuration of local glaciers, and with the exception of regional relative sea-level curves derived from raised marine deposits and isolation basins, do not provide large-scale constraints on EAIS changes. This situation is analogous to the McMurdo Dry Valleys, which have remained largely ice free for the past 14 Ma (Sugden et al., 1993) due to a low accumulation rate and the regional streaming of ice via major outlets such as the Byrd Glacier. In East Antarctica, Larsemann Hills, Bunger Hills and perhaps Vestfold Hills are in this category. While the major ice streams located adjacent to these ice-free areas may have thickened and expanded onto the continental shelf at the LGM, they did not necessarily penetrate the adjacent ice-free regions, which are more influenced by local glaciers. Parts of the Larsemann Hills most likely remained ice free during the LGM (Hodgson et al., 2001) and Vestfold Hills were also perhaps not completely covered by ice at the LGM (Gibson et al., 2009). This is despite relative-sea level data indicating additional regional ice loading at the time (Zwartz et al., 1998; Verleyen et al., 2005), and evidence for an expansion of grounded ice on the continental shelf (Domack et al., 1998). A similar situation existed at Bunger Hills, which remained largely ice free at the LGM (Gore et al., 2001).

In summary, evidence of the LGM extent and thickness of the EAIS remains poorly documented, and is lacking for the majority of the East Antarctic continental margin. Available evidence indicates that the LGM ice sheet was thinner in its centre, and in some areas thickened near the coast, expanding significantly onto the continental shelf. These geometrical constraints require an ice sheet with a low surface gradient, especially over continental shelf areas where ice streams were active (e.g. Mackintosh et al., 2011; White et al., 2011b). Despite these broad controls, we note that previous regional-scale estimates of the extent of grounded ice (Anderson et al., 2002; Livingstone et al., 2012) (Fig. 1) around the periphery of the EAIS, including most of Dronning Maud Land and Wilkes Land, are largely speculative. We recommend that ice sheet modellers focus on areas where constraints are strong (e.g. Golledge et al., 2012; Whitehouse et al., 2012), and that they recognise the uncertainty (and thus latitude) that exists in remaining areas.

We urge the geological community to target the many regions of the ice sheet where data are lacking. In particular, more chronological work is required. For example, further TCN dating of erratic boulders in Dronning Maud Land should be carried out. Lack of ice-thickness data from regions such as George V Land and Wilkes Land for the LGM and Holocene mean that glacio-isostatic adjustment (GIA) estimates are highly uncertain in these areas, limiting our ability to understand present-day ice sheet changes using data from the GRACE mission (King et al., 2012).

## 5.2. What was the timing of maximum ice extent, and subsequent retreat?

Constraint on the timing of the LGM and subsequent retreat history of the EAIS comes from TCN dating of glacial erratics in ice-free oases, marine  $^{14}\text{C}$  ages from sedimentary deposits on the continental shelf, and  $^{14}\text{C}$  and luminescence dates from terrestrial deposits (Fig. 8; Supplementary data table). Unfortunately dating control is not yet strong enough to attempt a time-slice reconstruction of EAIS deglaciation. The earliest evidence of ice sheet retreat comes from a handful of TCN ages in the Prince Charles Mountains that indicate retreat in the Lambert/Amery system may have begun as early as 18 ka ago (White et al., 2011b). At this site, as well as in the Adélie Basin, ice sheet retreat was perhaps nearly completed by ~12 ka ago. At Nielsen Basin in Mac.Robertson Land, deglaciation began by ~14 ka BP, but at many other sites documented in this review (Fig. 8), including Lützow-Holm Bay, Iceberg Alley, Framnes Mountains, Svenner Channel, and Windmill Islands, ice retreat most likely began at ~12 ka BP and continued into the Holocene. This delayed onset to deglaciation has also been documented at a number of other sites around both West and East Antarctic ice sheets (Mackintosh et al., 2011).

Based on available age constraints, we tentatively suggest that the EAIS responded in the following manner during the LGM and the transition to the Holocene: (1) The ice sheet was generally more extensive than present during the global LGM (~27–20 ka BP) (Clark et al., 2009); (2) Onset of ice sheet retreat began as early as 18 ka BP in the Lambert/Amery system, perhaps due to an enhanced sensitivity (Golledge et al., 2012) to an abrupt post-glacial sea-level rise at this time; (3) Retreat occurred at some sites at ~14 ka BP, coinciding with MWP1a. This apparent far-field response to the sea-level rise may also have occurred in West Antarctica and on the Antarctic Peninsula (Heroy and Anderson, 2007; Mackintosh et al., 2011); (4) The majority of ice sheet retreat occurred at the onset of the Holocene (~12 ka BP), in response to oceanic warming (Mackintosh et al., 2011), coinciding with the Early Holocene warm period recorded in ice cores and lake sediment records (Verleyen et al., 2011); (5) The ice sheet reached its present-day extent by the middle Holocene (e.g. Goodwin, 1993; Mackintosh et al., 2007; Yamane et al., 2011). This five-stage model of EAIS response is a hypothesis, and requires further testing.

We urge the geological community to target East Antarctic sites for dating, especially nunataks and on the continental shelf. It is important to test the hypothesis that the EAIS for the most part maintained its LGM ice extent until after Northern Hemisphere ice sheet retreat began, as existing data are too sparse. Ice sheet modellers should aim to further understand the ice-dynamic controls that might have resulted in the spatially distinctive pattern of ice sheet retreat indicated by available data.

## 5.3. Did the East Antarctic Ice Sheet contribute to MWP1a?

MWP1a involved a sea-level rise of ~14–18 m between ~14.7 and 13.3 ka BP (Deschamps et al., 2012), and the spatial pattern of sea-level rise during this event suggests a significant meltwater contribution from the Southern Hemisphere (Clark et al., 2002). This is a problem because recent ice sheet models constrained by available geological and ice core data indicate that the total extra volume of ice locked up in the Antarctic ice sheet during the LGM was only ~10 m of eustatic sea-level equivalent, or less (Mackintosh et al., 2011; Golledge et al., 2012; Whitehouse et al., 2012).

Mackintosh et al. (2011) estimate that the volume of the EAIS excluding the marine embayments of the Ross and Weddell Seas increased by only ~1 m of eustatic sea-level equivalent at the LGM.



This is around 10% of the total contribution from Antarctica indicated by recent ice sheet models (Pollard and DeConto, 2009; Mackintosh et al., 2011; Golledge et al., 2012; Whitehouse et al., 2012). Given the small volume of ice available, and evidence that deglaciation for the most part started late and progressed slowly, it is difficult to understand how the EAIS might have contributed significantly to MWP1a. We note, however, that these models have not been adequately constrained in many parts of East Antarctica. Furthermore, a small contribution to MWP1a has been suggested from the Lambert/Amery system (Verleyen et al., 2005). To fully answer the question of whether the EAIS contributed to this event, our community needs to target sectors of the ice sheet where data are lacking (e.g. Enderby Land, onshore George V Land), or where dating control is poor (e.g. Dronning Maud Land, Wilkes Land). Replicate studies are also needed in the Prince Charles and Framnes Mountains, where important inferences are based on relatively few ages. Modelled ice volume contributions also need to be updated as new geological and ice core data becomes available.

## Acknowledgements

We acknowledge financial support from the Antarctic Climate Evolution (ACE) scientific research programme of the Scientific Committee on Antarctic Research (SCAR) for a workshop held in 2011 in Edinburgh (UK) that initiated the Antarctic Ice Sheet community reconstruction initiative. Mackintosh and Golledge acknowledge financial support from the VUW Foundation Grant 'Antarctic Research Centre Climate and Ice-Sheet Modelling'. Verleyen and Vyverman acknowledge financial support from BelSPO (Holant project) and the InBev-Baillet-Latour Fund. Crosta and Massé acknowledge financial support from ANR CLIMICE. We thank Pippa Whitehouse for providing modelled ice sheet elevations, David Pollard and Robert DeConto for discussion of their ice sheet model and Shaun Eaves for providing feedback on the manuscript. We also thank two anonymous reviewers and guest editor John Anderson for feedback that improved the manuscript.

## Appendix A. Supplementary data

Supplementary data related to this article can be found at <http://dx.doi.org/10.1016/j.quascirev.2013.07.024>.

## References

- Adamson, D.A., Colhoun, E.A., 1992. Late Quaternary glaciation and deglaciation of the Bunger Hills, Antarctica. *Antarctic Science* 4, 435–446.
- Altmair, M., Herpers, U., Delisle, G., Merchel, S., Ott, U., 2010. Glaciation history of Queen Maud Land (Antarctica) reconstructed from in-situ produced cosmogenic  $^{10}\text{Be}$ ,  $^{26}\text{Al}$  and  $^{21}\text{Ne}$ . *Polar Science* 4, 42–61.
- Anderson, J.B., Shipp, S.S., Lowe, A.L., Wellner, J.S., Mosola, A.B., 2002. The Antarctic Ice Sheet during the Last Glacial Maximum and its subsequent retreat history: a review. *Quaternary Science Reviews* 21, 49–70.
- Andrews, J.T., Domack, E.W., Cunningham, W.L., Leventer, A., Licht, K.J., Jull, A.J.T., DeMaster, D.J., Jennings, A.E., 1999. Problems and possible solutions concerning radiocarbon dating of surface marine sediments, Ross Sea, Antarctica. *Quaternary Research* 52, 206–216.
- Balco, G., 2009. CRONUS Online Cosmogenic-nuclide Calculator. Available at: <http://hess.ess.washington.edu/>.
- Balco, G., 2011. Contributions and unrealized potential contributions of cosmogenic-nuclide exposure dating to glacier chronology, 1990–2010. *Quaternary Science Reviews* 30, 3–27.
- Barbara, L., Crosta, X., Masse, G., Ther, O., 2010. Deglacial environments in eastern Prydz Bay, East Antarctica. *Quaternary Science Reviews* 29, 2731–2740.
- Bardin, V.I., 1982. Composition of East Antarctic moraines and some problems of Cenozoic history. In: Craddock, C. (Ed.), *Antarctic Geoscience*. Wisconsin Press, Madison, pp. 1069–1076.
- Barrett, P.J., 1996. Antarctic paleoenvironment through Cenozoic times – a review. *Terra Antarctica* 3, 103–119.
- Beaman, R.J., Harris, P.T., 2003. Seafloor morphology and acoustic facies of the George V Land shelf. *Deep-Sea Research* 50, 1343–1355.
- Beaman, R.J., O'Brien, P.E., Post, A.L., De Santis, L., 2011. A new high-resolution bathymetry model for the Terre Adelie and George V continental margin, East Antarctica. *Antarctic Science* 23, 95–103.
- Bentley, M.J., 1999. Volume of Antarctic ice at the Last Glacial Maximum, and its impact on global sea level change. *Quaternary Science Reviews* 18, 1569–1596.
- Bentley, M.J., Fogwill, C.J., Kubik, P.W., Sugden, D.E., 2006. Geomorphological evidence and cosmogenic  $^{10}\text{Be}/^{26}\text{Al}$  exposure ages for the Last Glacial Maximum and deglaciation of the Antarctic Peninsula Ice Sheet. *Geological Society of America Bulletin* 118, 1149–1159.
- Berg, S., Wagner, B., White, D.A., Cremer, H., Bennike, O., Melles, M., 2009. Short note: new marine core record of Late Pleistocene glaciation history, Rauer Group, East Antarctica. *Antarctic Science* 21, 299–300.
- Berg, S., Wagner, B., Cremer, H., Leng, M.J., Melles, M., 2010a. Late Quaternary environmental and climate history of Rauer Group, East Antarctica. *Palaeogeography, Palaeoclimatology, Palaeoecology* 297, 201–213.
- Berg, S., Wagner, B., White, D., Melles, M., 2010b. No significant ice-sheet expansion beyond present ice margins during the past 4500 yr at Rauer Group, East Antarctica. *Quaternary Research* 74, 23–25.
- Berkman, P.A., Forman, S.L., 1996. Pre-bomb radiocarbon and the reservoir correction for calcareous marine species in the southern ocean. *Geophysical Research Letters* 23, 363–366.
- Burgess, J., Spate, A., Shevlin, J., 1994. The onset of deglaciation in the Larsemann Hills, eastern Antarctica. *Antarctic Science* 6, 491–495.
- Clark, C.D., 1993. Mega-scale glacial lineations and cross-cutting ice-flow landforms. *Earth Surface Processes and Landforms* 18, 1–29.
- Clark, P.U., Dyke, A.S., Shakun, J.D., Carlson, A.E., Clark, J., Wohlfarth, B., Mitrovica, J.X., Hostetler, S.W., McCabe, A.M., 2009. The Last Glacial Maximum. *Science* 325, 710–714.
- Clark, P.U., Mitrovica, J.X., Milne, G.A., Tamisiea, M.E., 2002. Sea-level fingerprinting as a direct test for the source of global Meltwater Pulse 1A. *Science* 295, 2438–2441.
- Colhoun, E.A., Adamson, D.A., 1989. Former glacial lakes of the Bunger Hills, Antarctica. *Australian Geographer* 20, 125–135.
- Colhoun, E.A., Mabin, M.C.G., Adamson, D.A., Kirk, R.M., 1992. Antarctic ice volume and contribution to sea-level fall at 20,000 yr BP from raised beaches. *Nature* 358, 316–319.
- Cremer, H., Gore, D., Melles, M., Roberts, D., 2003. Palaeoclimatic significance of late Quaternary diatom assemblages from southern Windmill Islands, East Antarctica. *Palaeogeography, Palaeoclimatology, Palaeoecology* 195, 261–280.
- Crosta, X., Debret, M., Denis, D., Courty, M.A., Ther, O., 2007. Holocene long- and short-term climate changes off Adélie Land, East Antarctica. *Geochemistry, Geophysics, Geosystems* 8, Q11009.
- Damm, V., 2007. A subglacial topographic model of the southern drainage area of the Lambert Glacier/Amery Ice Shelf System. Results of an Airborne Ice Thickness Survey South of the Prince Charles Mountains. *Terra Antarctica* 14, 85–94.
- Delmotte, M., Raynaud, D., Morgan, V., Jouzel, J., 1999. Climatic and glaciological information inferred from air-content measurements of a Law Dome (East Antarctica) ice core. *Journal of Glaciology* 45, 255–263.
- Denis, D., Crosta, X., Schmidt, S., Carson, D.S., Ganeshram, R.S., Renssen, H., Bout-Roumazilles, V., Zaragosi, S., Martin, B., Cremer, M., Giraudeau, J., 2009. Holocene glacier and deep water dynamics, Adelie Land region, East Antarctica. *Quaternary Science Reviews* 28, 1291–1303.
- Deschamps, P., Durand, N., Bard, E., Hamelin, B., Camoin, G., Thomas, A.L., Henderson, G.M., Okuno, J., Yokoyama, Y., 2012. Ice-sheet collapse and sea-level rise at the Bolling warming 14,600 years ago. *Nature* 483, 559–564.
- Domack, E., 1982. Sedimentology of glacial and glacial-marine deposits of the George V-Adelie continental shelf. *Boreas* 11, 79–97.
- Domack, E., O'Brien, P., Harris, P., Taylor, F., Quilty, P., De Santis, L., Raker, B., 1998. Late Quaternary sediment facies in Prydz Bay, East Antarctica and their relationship to glacial advance onto the continental shelf. *Antarctic Science* 10, 236–246.
- Domack, E.W., Jacobson, E.A., Shipp, S.S., Anderson, J.B., 1999. Late Pleistocene/Holocene retreat of the West Antarctic Ice Sheet in the Ross Sea: part 2—sedimentologic and stratigraphic signature. *Geological Society of America Bulletin* 111, 1517–1536.
- Domack, E.W., Jull, A.J.T., Anderson, J.B., Linick, T.W., Williams, C.R., 1989. Application of tandem accelerator mass-spectrometer dating to late Pleistocene–Holocene sediments of the East Antarctic continental shelf. *Quaternary Research* 31, 277–287.
- Domack, E.W., Jull, A.J.T., Nakao, S., 1991. Advance of East Antarctic outlet glaciers during the hypsithermal; implications for the volume state of the Antarctic ice sheet under global warming. *Geology* 19, 1059–1062.
- Dowdeswell, J.A., Fugelli, E.M.G., 2012. The seismic architecture and geometry of grounding-zone wedges formed at the marine margins of past ice sheets. *Geological Society of America Bulletin* 124, 1750–1761.
- Eittrheim, S.L., Cooper, A.K., Wamnesson, J., 1995. Seismic stratigraphic evidence of ice-sheet advances on the Wilkes Land margin of Antarctica. *Sedimentary Geology* 96, 131–156.
- Elverhoi, A., 1981. Evidence for a Late Wisconsin glaciation of the Weddell Sea. *Nature* 293, 641–642.
- Engelskjön, T., 1986. Botany of two Antarctic mountain ranges: Gjelsvikfjella and Mühlig-Hofmannfjella, Dronning Maud Land. I. General ecology and development of the Antarctic cold desert cryptogam formation. *Polar Research* 4, 205–224.
- Escutia, C., Brinkhuis, H., Klaus, A., Expedition\_318\_Scientists, 2011. Proceedings of the Integrated Ocean Drilling Program 318. Integrated Ocean Drilling Program Management International, Tokyo.

- Escutia, C., Warnke, D., Acton, G.D., Barcena, A., Burckle, L., Canals, M., Frazee, C.S., 2003. Sediment distribution and sedimentary processes across the Antarctic Wilkes Land margin during the Quaternary. *Deep Sea Research Part II: Topical Studies in Oceanography* 50, 1481–1508.
- Fabel, D., Stone, J.O., Fifield, L.K., Cresswell, I.R.G., 1997. Deglaciation of the Vestfold Hills, East Antarctica: preliminary evidence from exposure dating of three sub-glacial erratics. In: Ricci, C.A. (Ed.), *The Antarctic Region: Geological Evolution and Processes*, Proceedings 7th International Symposium on Antarctic Earth Science, Siena, pp. 829–834.
- Fink, D., McKelvey, B., Hambrey, M., Fabel, D., Brown, R., 2006. Pleistocene deglaciation chronology of the Amery Oasis and Radok Lake, northern Prince Charles Mountains, Antarctica. *Earth and Planetary Science Letters* 243, 229–243.
- Fink, D., Smith, A.M., 2007. An inter-comparison of  $^{10}\text{Be}$  and  $^{26}\text{Al}$  AMS reference standards and the  $^{10}\text{Be}$  half-life. *Nuclear Instruments and Methods in Physics Research Section B: Beam Interactions with Materials and Atoms* 259, 600–609.
- Flower, B.P., Kennett, J.P., 1994. The middle Miocene climatic transition: east Antarctic ice sheet development, deep ocean circulation and global carbon cycling. *Palaeogeography, Palaeoclimatology, Palaeoecology* 108, 537–555.
- Fretwell, P., Pritchard, H.D., Vaughan, D.G., Bamber, J.L., Barrand, N.E., Bell, R., Bianchi, C., Bingham, R.G., Blankenship, D.D., Casassa, G., Catania, G., Callens, D., Conway, H., Cook, A.J., Corr, H.F.J., Damaske, D., Damm, V., Ferraccioli, F., Forsberg, R., Fujita, S., Gim, Y., Gogineni, P., Griggs, J.A., Hindmarsh, R.C.A., Holmlund, P., Holt, J.W., Jacobel, R.W., Jenkins, A., Jokat, W., Jordan, T., King, E.C., Kohler, J., Krabill, W., Riger-Kusk, M., Langley, K.A., Leitchenkov, G., Leuschen, C., Luyendyk, B.P., Matsuoka, K., Mouginit, J., Nitsche, F.O., Nogi, Y., Nost, O.A., Popov, S.V., Rignot, E., Rippin, D.M., Rivera, A., Roberts, J., Ross, N., Siegert, M.J., Smith, A.M., Steinhage, D., Studinger, M., Sun, B., Tinto, B.K., Welch, B.C., Wilson, D., Young, D.A., Xiangbin, C., Zirizzotti, A., 2013. Bedmap2: improved ice bed, surface and thickness datasets for Antarctica. *The Cryosphere* 7, 375–393.
- Gibson, J., Paterson, K., White, C., Swadling, K., 2009. Evidence for the continued existence of Abraxas Lake, Vestfold Hills, East Antarctica during the Last Glacial Maximum. *Antarctic Science* 21, 269–278.
- Gingele, F., Kuhn, G., Maus, B., Melles, M., Schöne, T., 1997. Sedimentology of cores from the shelf of Lazarev Sea, East Antarctica. *Continental Shelf Research* 17, 137–163.
- Golledge, N.R., Fogwill, C.J., Mackintosh, A.N., Buckley, K.M., 2012. Dynamics of the last glacial maximum Antarctic ice-sheet and its response to ocean forcing. *Proceedings of the National Academy of Sciences* 109, 16052–16056.
- Goode, J.W., Fanning, C.M., 2010. Composition and age of the East Antarctic Shield in eastern Wilkes Land determined by proxy from Oligocene–Pleistocene glaciomarine sediment and Beacon Supergroup sandstones, Antarctica. *Geological Society of America Bulletin* 122, 1135–1159.
- Goodwin, I.D., 1993. Holocene deglaciation, sea-level change, and the emergence of the Windmill Islands, Budd Coast, Antarctica. *Quaternary Research* 40, 70–80.
- Goodwin, I.D., 1996. Evidence for a Late Holocene readvance of the Law Dome, East Antarctica. *Antarctic Science* 8, 395–406.
- Goodwin, I.D., 1998. Did changes in Antarctic ice volume influence Late Holocene sea-level lowering? *Quaternary Science Reviews* 17, 319–332.
- Goodwin, I.D., Zweck, C., 2000. Glacio-isostasy and glacial ice load at Law Dome, Wilkes Land, East Antarctica. *Quaternary Research* 53, 285–293.
- Gordon, J.E., Harkness, D.D., 1992. Magnitude and geographic variation of the radiocarbon content in Antarctic marine life: implications for reservoir corrections in radiocarbon dating. *Quaternary Science Reviews* 11, 697–708.
- Gore, D.B., 1997. Blanketing snow and ice: constraints on radiocarbon dating deglaciation in East Antarctic oases. *Antarctic Science* 9, 336–348.
- Gore, D.B., Colhoun, E.A., Bell, K., 1994. Derived constituents in the glacial sediments of the Vestfold Hills, East Antarctica. *Quaternary Science Reviews* 13, 301–307.
- Gore, D.B., Creagh, D.C., Burgess, J.S., Colhoun, E.A., Spate, A.P., Baird, A.S., 1996. Composition, distribution and origin of surficial salts in the Vestfold Hills, East Antarctica. *Antarctic Science* 8, 73–84.
- Gore, D.B., Rhodes, E.J., Augustinus, P.C., Leishman, M.R., Colhoun, E.A., Rees-Jones, J., 2001. Bunge Hills, East Antarctica: ice free at the Last Glacial Maximum. *Geology* 29, 1103–1106.
- Gore, D.B., Snape, I., Leishman, M., 2003. Glacial sediment provenance, dispersal and deposition, Vestfold Hills, East Antarctica. *Antarctic Science* 15, 259–269.
- Hall, B.L., Henderson, G.M., Baroni, C., Kellogg, T.B., 2010. Constant Holocene Southern-Ocean  $^{14}\text{C}$  reservoir ages and ice-shelf flow rates. *Earth and Planetary Science Letters* 296, 115–123.
- Harris, P.T., Beaman, R.J., 2003. Processes controlling the formation of the Mertz Drift, George Vth continental shelf, East Antarctica: Evidence from 3.5 kHz sub-bottom profiling and sediment cores. *Deep-Sea Research* 50, 1463–1480.
- Harris, P.T., Brancolini, G., Armand, L., Busetti, M., Beaman, R.J., Giorgetti, G., Presti, M., Trincardi, F., 2001. Continental shelf drift deposit indicates non-steady state Antarctic bottom water production in the Holocene. *Marine Geology* 179, 1–8.
- Harris, P.T., O'Brien, P.E., 1998. Bottom currents, sedimentation and ice-sheet retreat facies successions on the Mac Robertson shelf, East Antarctica. *Marine Geology* 151, 47–72.
- Harris, P.T., Taylor, F., Domack, E., DeSantis, L., Goodwin, I., Quilty, P.G., O'Brien, P.E., 1997. Glaciomarine siliciclastic muds from Vincennes Bay, East Antarctica: preliminary results of an exploratory cruise in 1997. *Terra Antarctica* 4, 11–20.
- Hattestrand, C., Johansen, N., 2005. Supraglacial moraines in Scharffenbergbotnen, Heimefrontfjella, Dronning Maud Land, Antarctica – significance for reconstructing former blue ice areas. *Antarctic Science* 17, 225–236.
- Hemer, M.A., Harris, P.T., 2003. Sediment core from beneath the Amery Ice Shelf, East Antarctica, suggests mid-Holocene ice-shelf retreat. *Geology* 31, 127–130.
- Hemer, M.A., Post, A.L., O'Brien, P.E., Craven, M., Truswell, E.M., Roberts, D., Harris, P.T., 2007. Sedimentological signatures of the sub-Amery Ice Shelf circulation. *Antarctic Science* 19, 497–506.
- Heroy, D.C., Anderson, J.B., 2007. Radiocarbon constraints on Antarctic Peninsula Ice Sheet retreat following the Last Glacial Maximum (LGM). *Quaternary Science Reviews* 26, 3286–3297.
- Hiller, A., Hermichen, W.-D., Wand, U., 1995. Radiocarbon-dated subfossil stomach oil deposits from petrel nesting sites: novel paleoenvironmental records from continental Antarctica. *Radiocarbon* 37, 171–180.
- Hiller, A., Wand, U., Kampf, H., Stackedbrandt, W., 1988. Occupation of the Antarctic continent of by petrels during the past 35000 years – inferences from a  $^{14}\text{C}$  study of stomach oil deposits. *Polar Biology* 9, 69–77.
- Hodgson, D.A., McMinn, A., Kirkup, H., Cremer, H., Gore, D., Melles, M., Roberts, D., Montiel, P., 2003. Colonization, succession, and extinction of marine floras during a glacial cycle: a case study from the Windmill Islands (east Antarctica) using biomarkers. *Paleoceanography* 18, 1067.
- Hodgson, D.A., Noon, P.E., Vyverman, W., Bryant, C.L., Gore, D.B., Appleby, P., Gilmour, M., Verleyen, E., Sabbe, A., Jones, V.J., Ellis-Evans, J.C., Wood, P.B., 2001. Were the Larsemann Hills ice-free through the Last Glacial Maximum? *Antarctic Science* 13, 440–454.
- Hodgson, D.A., Verleyen, E., Sabbe, K., Squier, A.H., Keely, B.J., Leng, M.J., Saunders, K.M., Vyverman, W., 2005. Late Quaternary climate-driven environmental change in the Larsemann Hills, East Antarctica, multi-proxy evidence from a lake sediment core. *Quaternary Research* 64, 83–99.
- Hodgson, D.A., Roberts, D., McMinn, A., Verleyen, E., Terry, B., Corbett, C., Vyverman, W., 2006a. Recent rapid salinity rise in three East Antarctic lakes. *Journal of Paleolimnology* 36, 385–406.
- Hodgson, D.A., Verleyen, E., Squier, A.H., Sabbe, K., Keely, B.J., Saunders, K.M., Vyverman, W., 2006b. Interglacial environments of coastal east Antarctica: comparison of MIS 1 (Holocene) and MIS 5e (Last Interglacial) lake-sediment records. *Quaternary Science Reviews* 25, 179–197.
- Huang, T., Sun, L., Wang, Y., Liu, X., Zhu, R., 2009. Penguin population dynamics for the past 8500 years at Gardner Island, Vestfold Hills. *Antarctic Science* 21, 571–578.
- Hughes, T., 2002. Calving bays. *Quaternary Science Reviews* 21, 267–282.
- Igarashi, A., Numanami, H., Tsuchiya, Y., Fukuchi, M., 2001. Bathymetric distribution of fossil foraminifera within marine sediment cores from the eastern part of Lützow-Holm Bay, East Antarctica, and its paleoceanographic implications. *Marine Micropaleontology* 42, 125–162.
- Ingólfsson, O., Hjort, C., Berkham, P.A., Björck, S., Colhoun, E., Goodwin, I.D., Hall, B., Hirakawa, K., Melles, M., Möller, P., Prentice, M.L., 1998. Antarctic glacial history since the Last Glacial Maximum: an overview of the record on land. *Antarctic Science* 10, 326–344.
- IPCC, 2007. *Climate Change 2007: the Physical Science Basis*. Cambridge University Press, Cambridge, United Kingdom and New York, NY, USA.
- Ishizuka, H., Shiraishi, K., Moriwaki, K., 1993. *Geological Map of Bergersenfjella*. In: *Antarctic Geological Map Series*. National Institute for Polar Research, Tokyo.
- Jonsson, S., 1988. *Observations on the Physical Geography and Glacial History of the Vestfjella Nunataks in Western Dronning Maud Land, Antarctica*. Department of Physical Geography, Stockholm University, p. 57. Research Report 68.
- Joughin, I., Alley, R.B., 2011. Stability of the West Antarctic ice sheet in a warming world. *Nature Geoscience* 4, 506–513.
- Jouzel, J., Raisbeck, G., Benoist, J.P., Yiou, F., Lorius, C., Raynaud, D., Petit, J.R., Barkov, N.I., Korotkevitch, Y.S., Kotlyakov, V.M., 1989. A comparison of deep Antarctic ice cores and their implications for climate between 65,000 and 15,000 years ago. *Quaternary Research* 31, 135–150.
- Kämpf, H., Stackedbrandt, W., Hahne, K., Paech, H.-J., Lepin, V.S., 1995. Wohlthat Massif. In: Bormann, P., Fritzsche, D. (Eds.), *The Schirmacher Oasis, Queen Maud Land, and its Surroundings*. Perthes, Gotha, pp. 133–152.
- Kiernan, K., Gore, D.B., Fink, D., White, D.A., McConnell, A., Sigurdsson, I., 2007. Deglaciation and weathering of Larsemann Hills, East Antarctica. *Antarctic Science* 21, 373–382.
- King, M.A., Bingham, R.J., Moore, P., Whitehouse, P.L., Bentley, M.J., Milne, G.A., 2012. Lower satellite-gravimetry estimates of Antarctic sea-level contribution. *Nature* 491, 586–589.
- Kirkup, H., Melles, M., Gore, D.B., 2002. Late Quaternary environment of southern Windmill Islands, East Antarctica. *Antarctic Science* 14, 385–394.
- Krause, W.E., Krbetschek, M.R., Stolz, W., 1997. Dating of Quaternary lake sediments from the Schirmacher oasis (East Antarctica) by infra-red stimulated luminescence (IRSL) detected at the wavelength of 560 nm. *Quaternary Science Reviews* 16, 387–392.
- Kulbe, T., Melles, M., Verkulich, S.R., Pushina, Z.V., 2001. East Antarctic climate and environmental variability over the last 9400 years inferred from marine sediments of the Bunge Oasis. *Arctic, Antarctic, and Alpine Research* 33, 223–230.
- Leventer, A., Domack, E., Dunbar, R., Pike, J., Stickley, C., Maddison, E., Brachfeld, S., Manley, P., McClennen, C., 2006. Marine sediment record from the East Antarctic margin reveals dynamics of ice sheet recession. *GSA Today* 16, 4–10.
- Lilly, K., Fink, D., Fabel, D., Lambeck, K., 2010. Pleistocene dynamics of the interior East Antarctic ice sheet. *Geology* 38, 703–706.
- Lintinen, P., 1996. Evidence for the former existence of a thicker ice sheet on the Vestfjella nunataks in western Dronning Maud Land, Antarctica. *Bulletin of the Geological Society of Finland* 68, 85–98.
- Lintinen, P., Nenonen, J., 1997. Glacial history of the Vestfjella and Heimefrontfjella nunatak ranges in western Dronning Maud Land, Antarctica. In: Ricci, C.A. (Ed.),

- The Antarctic Region: Geological Evolution and Processes. Terra Antarctica Publications, Siena, pp. 845–852.
- Livingstone, S.J., O'Cofaigh, C., Stokes, C.R., Hillenbrand, C.-D., Vieli, A., Jamieson, S.S.R., 2012. Antarctic palaeo-ice streams. *Earth-Science Reviews* 111, 90–128.
- Lorius, C., Raynaud, D., Petit, J.R., Jouzel, J., Merlivat, L., 1984. Late Glacial Maximum-Holocene atmospheric and ice-thickness changes from Antarctic ice-core studies. *Annals of Glaciology* 5, 88–94.
- Lythe, M.B., Vaughan, D.G., the, B.C., 2001. BEDMAP: a new ice thickness and sub-glacial topographic model of Antarctica. *J. Geophys. Res.* 106, 11335–11351.
- Mabin, M.C.G., 1991. The glacial history of the Lambert Glacier/Prince Charles Mountains area and comparisons with the record from the Transantarctic Mountains. In: Gillieson, D., Fitzsimons, S. (Eds.), *Quaternary Research in Australian Antarctica*. Department of Geography and Oceanography. Australian Defence Force Academy, Canberra, pp. 15–23.
- Mackintosh, A., Gollède, N., Domack, E., Dunbar, R., Leventer, A., White, D., Pollard, D., DeConto, R., Fink, D., Zwart, D., Gore, D., Lavoie, C., 2011. Retreat of the East Antarctic ice sheet during the last glacial termination. *Nature Geoscience* 4, 195–202.
- Mackintosh, A., White, D., Fink, D., Gore, D.B., Pickard, J., Fanning, P.C., 2007. Exposure ages from mountain dipsticks in MacRobertson Land, East Antarctica, indicate little change in ice-sheet thickness since the Last Glacial Maximum. *Geology* 35, 551–554.
- Maddison, E.J., Pike, J., Dunbar, R., 2012. Seasonally laminated diatom-rich sediments from Dumont d'Urville Trough, East Antarctic Margin: Late-Holocene Neoglacial sea-ice conditions. *The Holocene* 22, 857–875.
- Matsuoka, N., Thomachot, C.E., Oguchi, C.T., Hattai, T., Abe, M., Matsuzaki, H., 2006. Quaternary bedrock erosion and landscape evolution in the Sør Rondane Mountains, East Antarctica: reevaluating rates and processes. *Geomorphology* 81 (3–4), 408–420. <http://dx.doi.org/10.1016/j.geomorph.2006.05.005>.
- McCormac, F.G., Hogg, A.G., Blackwell, P.G., Buck, C.E., Higham, T.F.G., Reimer, P.J., 2004. SHCal04—Southern Hemisphere calibration, 0–11.0 cal kyr BP. *Radiocarbon* 46 (3), 1087–1092.
- McKay, R.M., Dunbar, G.B., Naish, T.R., Barrett, P.J., Carter, L., Harper, M., 2008. Retreat history of the Ross Ice Sheet (Shelf) since the Last Glacial Maximum from deep-basin sediment cores around Ross Island. *Palaeogeography, Palaeoclimatology, Palaeoecology* 260, 245–261.
- McMullen, K., Domack, E., Leventer, A., Olson, C., Dunbar, R., Brachfeld, S., 2006. Glacial morphology and sediment formation in the Mertz Trough, East Antarctica. *Palaeogeography, Palaeoclimatology, Palaeoecology* 231, 169–180.
- Melles, M., Verkulich, S.R., Hermichen, W., 1994. Radiocarbon dating of lacustrine and marine sediments from the Bunge Hills, East Antarctica. *Antarctic Science* 6, 375–378.
- Miura, H., Maemoku, H., Seto, K., Moriwaki, K., 1998a. Late Quaternary East Antarctic melting event in the Soya Coast region based on stratigraphy and oxygen isotopic ratio of fossil molluscs. *Polar Geoscience* 11, 260–274.
- Miura, H., Moriwaki, K., Maemoku, H., Hirakawa, K., 1998b. Fluctuations of the East Antarctic ice-sheet margin since the last glaciation from the stratigraphy of raised beach deposits along the Soya Coast. *Annals of Glaciology* 27, 297–301.
- Moriwaki, K., Hirakawa, K., Hayashi, M., Iwata, S., 1992. Late Cenozoic Glacial History in the Sør Rondane Mountains, East Antarctica. In: Yoshida, Y., Kaminuma, K., Shiraiishi, K. (Eds.), *Recent Progress in Antarctic Earth Science*. Terra Scientific Publishing Company, Tokyo, pp. 661–668.
- Moriwaki, K., Hirakawa, K., Matsuoka, N., 1991. Weathering stage of till and glacial history of the central Sør Rondane Mountains, East Antarctica. *Proceedings of the NIPR Symposium on Antarctic Geoscience* 5, 99–111.
- Neethling, D.C., 1969. Geology of the Ahlmann Ridge, Western Queen Maud Land, Antarctic Map Folio Series. American Geographical Society.
- Nishiizumi, K., Imamura, M., Caffee, M.W., Southon, J.R., Finkel, R.C., McAninch, J., 2007. Absolute calibration of  $^{10}\text{Be}$  AMS standards. *Nuclear Instruments and Methods in Physics Research Section B: Beam Interactions with Materials and Atoms* 258, 403–413.
- Nishiizumi, K., Kohl, C.P., Arnold, J.R., Klein, J., Fink, D., Middleton, R., 1991. Cosmic ray produced  $^{10}\text{Be}$  and  $^{26}\text{Al}$  in Antarctic rocks: exposure and erosion history. *Earth and Planetary Science Letters* 104, 440–454.
- O'Brien, P., Leitchenkov, G., 1997. Deglaciation of Prydz Bay, East Antarctica, Based on Echo Sounding and Topographic Features, Geology and Seismic Stratigraphy of the Antarctic Margin, 2. AGU, Washington, DC, pp. 109–126.
- O'Brien, P.E., De Santis, L., Harris, P.T., Domack, E., Quilty, P.G., 1999. Ice shelf grounding zone features of western Prydz Bay, Antarctica: sedimentary processes from seismic and sidescan images. *Antarctic Science* 11, 78–91.
- O'Brien, P.E., Goodwin, I., Forsberg, C.F., Cooper, A.K., Whitehead, J., 2007. Late Neogene ice drainage changes in Prydz Bay, East Antarctica and the interaction of Antarctic ice sheet evolution and climate. *Palaeogeography, Palaeoclimatology, Palaeoecology* 245, 390–410.
- Parrenin, F., Barnola, J.M., Beer, J., Blunier, T., Castellano, E., Chappellaz, J., Dreyfus, G., Fischer, H., Fujita, S., Jouzel, J., Kawamura, K., Lemieux-Dudon, B., Loulergue, L., Masson-Delmotte, V., Narcisi, B., Petit, J.R., Raisbeck, G., Raynaud, D., Ruth, U., Schwander, J., Severi, M., Spahni, R., Steffensen, J.P., Svensson, A., Udisti, R., Waelbroeck, C., Wolff, E., 2007a. The EDC3 chronology for the EPICA Dome C ice core. *Climate of the Past* 3, 485–497.
- Parrenin, F., Dreyfus, G., Durand, G., Fujita, S., Gagliardini, O., Gillet, F., Jouzel, J., Kawamura, K., Lhomme, N., Masson-Delmotte, V., Ritz, C., Schwander, J., Shoji, H., Uemura, R., Watanabe, O., Yoshida, N., 2007b. 1-D-ice flow modelling at EPICA Dome C and Dome Fuji, East Antarctica. *Climate of the Past* 3, 243–259.
- Pattyn, F., Matsuoka, K., Berte, J., 2010. Glacio-meteorological conditions in the vicinity of the Belgian Princess Elisabeth Station, Antarctica. *Antarctic Science* 22, 79–85.
- Patzelt, G., 1988. Die Geowissenschaftliche Expedition in die Kottasberge/Heimefrontfjella und die Kralberge/Vestfjella – Glacialmorphologische Untersuchungen. In: Futterer, D.K. (Ed.), *Berichte zur Polarforschung*. Alfred Wegener Institut für Polar und Meeresforschung, Bremerhaven, Germany.
- Phartiyal, B., Sharma, A., Bera, S.K., 2011. Glacial lakes and geomorphological evolution of Schirmacher Oasis, East Antarctica, during Late Quaternary. *Quaternary International* 235, 128–136.
- Pickard, J., Adamson, D.A., Harwood, D.M., Miller, G.H., Quilty, P.G., Dell, R.K., 1988. Early Pliocene marine sediments, coastline, and climate of East Antarctica. *Geology* 16, 158–161.
- Pickard, J., Seppelt, R.D., 1984. Holocene occurrence of the moss *Bryum* algae in the Vestfold Hills, Antarctica. *Journal of Bryology* 13, 209–217.
- Pingree, K., Lurie, M., Hughes, T., 2011. Is the East Antarctic ice sheet stable? *Quaternary Research* 75, 417–429.
- Pollard, D., DeConto, R.M., 2009. Modelling West Antarctic ice sheet growth and collapse through the past five million years. *Nature* 458, 329–332.
- Presti, M., De Santis, L., Brancolini, G., Harris, P.T., 2005. Continental shelf record of the East Antarctic Ice Sheet evolution: seismo-stratigraphic evidence from the George V Basin. *Quaternary Science Reviews* 24, 1223–1241.
- Presti, M., De Santis, L., Busetti, M., Harris, P.T., 2003. Late Pleistocene and Holocene sedimentation on the George V Continental Shelf, East Antarctica. *Deep Sea Research Part II: Topical Studies in Oceanography* 50, 1441–1461.
- Pritchard, H.D., Arthern, R.J., Vaughan, D.G., Edwards, L.A., 2009. Extensive dynamic thinning on the margins of the Greenland and Antarctic ice sheets. *Nature* 461, 971–975.
- Reimer, P.J., Reimer, R.W., 2001. A marine reservoir correction database and on-line interface. *Radiocarbon* 43, 461–463.
- Reimer, P.J., Baillie, M.G.L., Bard, E., Bayliss, A., Beck, J.W., Blackwell, P.G., Bronk Ramsey, C., Buck, C.E., Burr, G.S., Edwards, R.L., Friedrich, M., Grootes, P.M., Guilderson, T.P., Hajdas, I., Heaton, T.J., Hogg, A.G., Hughes, K.A., Kaiser, K.F., Kromer, B., McCormac, F.G., Manning, S.W., Reimer, R.W., Richards, D.A., Southon, J.R., Talamo, S., Turney, C.S.M., van der Plicht, J., Weyhenmeyer, C.E., 2009. IntCal09 and Marine09 radiocarbon age calibration curves, 0–50,000 years cal BP. *Radiocarbon* 51 (4), 1111–1150.
- Richter, W., Bormann, P., 1995. Geomorphology. In: Bormann, P., Fritzsche, D. (Eds.), *The Schirmacher Oasis, Queen Maud Land, and Its Surroundings*. Perthes, Gotha, pp. 171–206.
- Rignot, E., Jacobs, S., Mouginot, J., Scheuchl, B., 2013. Ice shelf melting around Antarctica. *Science* 333 (6048), 1427–1430.
- Rignot, E., Mouginot, J., Scheuchl, B., 2011. Ice flow of the Antarctic Ice Sheet. *Science* 333, 1427–1430.
- Roberts, D., McMinn, A., Cremer, H., Gore, D.B., Melles, M., 2004. The Holocene evolution and palaeosalinity history of Beall Lake, Windmill Islands (East Antarctica) using an expanded diatom-based weighted averaging model. *Palaeogeography, Palaeoclimatology, Palaeoecology* 208, 121–140.
- Roberts, D., McMinn, A., Zwart, D., 2000. An initial palaeosalinity history of Jaw Lake, Bunge Hills based on a diatom-salinity transfer function applied to sediment cores. *Antarctic Science* 12, 172–176.
- Sedwick, P.N., Harris, P.T., Robertson, L.G., McMurtry, G.M., Cremer, M.D., Robinson, P., 1998. A geochemical study of marine sediments from the MacRobertson shelf, East Antarctica: initial results and palaeoenvironmental implications. *Annals of Glaciology* 27, 268–274.
- Sedwick, P.N., Harris, P.T., Robertson, L.G., McMurtry, G.M., Cremer, M.D., Robinson, P., 2001. Holocene sediment records from the continental shelf of MacRobertson Land, East Antarctica. *Palaeogeography* 16, 212–225.
- Shepherd, A., Ivins, E.R., A., G., Barletta, V.R., Bentley, M.J., Bettadpur, S., Briggs, K.H., Bromwich, D.H., Forsberg, R., Galin, N., Horwath, M., Jacobs, S., Joughin, I., King, M.A., Lenaerts, J.T.M., Li, J., Lichtenberg, S.R.M., Luckman, A., Luthcke, S.B., McMillan, M., Meister, R., Milne, G., Mouginot, J., Muir, A., Nicolas, J.P., Paden, J., Payne, A.J., Pritchard, H., Rignot, E., Rott, H., Sørensen, L.S., Scambos, T.A., Scheuchl, B., Schrama, E.J.O., Smith, B., Sundal, A.V., van Angelen, J.H., van de Berg, W.J., van den Broeke, M.R., Vaughan, D.G., Velicogna, I., Wahr, J., Whitehouse, P.L., Wingham, D.J., Yi, D., Young, D., Zwally, H.J., 2012. A reconciled estimate of ice-sheet mass balance. *Science* 338, 1183–1189.
- Shipp, S., Anderson, J., Domack, E., 1999. Late Pleistocene–Holocene retreat of the West Antarctic Ice-Sheet system in the Ross Sea: part 1 – geophysical results. *Geological Society of America Bulletin* 111, 1486–1516.
- Siddall, M., Milne, G.A., Masson-Delmotte, V., 2012. Uncertainties in elevation changes and their impact on Antarctic temperature records since the end of the last glacial period. *Earth and Planetary Science Letters* 315 (Ä316), 12–23.
- Simms, A.R., DeWitt, R., Kouremenos, P., Drewry, A.M., 2011. A new approach to reconstructing sea levels in Antarctica using optically stimulated luminescence of cobble surfaces. *Quaternary Geochronology* 6, 50–60.
- Steele, W.K., Hiller, A., 1997. Radiocarbon dates of snow petrel (*Pagodroma nivea*) nest sites in central Dronning Maud Land, Antarctica. *Polar Record* 33, 29–38.
- Stone, J.O., Balco, G.A., Sugden, D.E., Caffee, M.W., Sass, L.C., Cowdery, S.G., Siddoway, C., 2003. Holocene deglaciation of Marie Byrd Land, West Antarctica. *Science* 299, 99–102.
- Stuiver, M., Reimer, P.J., 1993. Extended  $^{14}\text{C}$  data base and revised CALIB 3.0  $^{14}\text{C}$  age calibration program. *Radiocarbon* 35, 215–230. CALIB 6.1.1 is available at: <http://calib.qub.ac.uk/calib/>.



- Sugden, D.E., Marchant, D.R., Denton, G.H., 1993. The case for a stable east Antarctic Ice Sheet: the background. *Geografiska Annaler. Series A, Physical Geography* 75, 151–154.
- Takada, M., Tani, A., Miura, H., Moriwaki, K., Nagatomo, T., 2003. ESR dating of fossil shells in the Lützow-Holm Bay region, East Antarctica. *Quaternary Science Reviews* 22, 1323–1328.
- Thor, G., Low, M., 2011. The persistence of the snow petrel (*Pagodroma nivea*) in Dronning Maud Land (Antarctica) for over 37,000 years. *Polar Biology* 34, 609–613.
- Verkulich, S., Melles, M., Hubberten, H.-W., Pushina, Z., 2002. Holocene environmental changes and development of Figurnoye Lake in the southern Bunger Hills, East Antarctica. *Journal of Paleolimnology* 28, 253–267.
- Verkulich, S.R., Hiller, A., 1994. Holocene deglaciation of the Bunger Hills revealed by  $^{14}\text{C}$  measurements on stomach oil deposits in snow petrel colonies. *Antarctic Science* 6, 395–399.
- Verleyen, E., Hodgson, D.A., Milne, G.A., Sabbe, K., Vyverman, W., 2005. Relative sea-level history from the Lambert Glacier region, East Antarctica, and its relation to deglaciation and Holocene glacier readvance. *Quaternary Research* 63, 45–52.
- Verleyen, E., Hodgson, D.A., Sabbe, K., Cremer, H., Emslie, S.D., Gibson, J., Hall, B., Imura, S., Kudoh, S., Marshall, G.J., McMinn, A., Melles, M., Newman, L., Roberts, D., Roberts, S.J., Singh, S.M., Sterken, M., Tavernier, I., Verkulich, S., Van de Vyver, E., Van Nieuwenhuize, W., Wagner, B., Vyverman, W., 2011. Post-glacial regional climate variability along the East Antarctic coastal margin—evidence from shallow marine and coastal terrestrial records. *Earth-Science Reviews* 104, 199–212.
- Wagner, B., Cremer, H., Hultsch, N., Gore, D., Melles, M., 2004. Late Pleistocene and Holocene history of Lake Terrasovoje, Amery Oasis, East Antarctica, and its climatic and environmental implications. *Journal of Paleolimnology* 32, 321–339.
- White, D., Hermichen, W., 2007. Glacial and Periglacial History of the Southern Prince Charles Mountains, East Antarctica. *Terra Antarctica* 14, 5–12.
- White, D.A., Bennike, O., Berg, S., Harley, S.L., Fink, D., Kiernan, K., McConnell, A., Wagner, B., 2009. Geomorphology and glacial history of Rauer Group, East Antarctica. *Quaternary Research* 72, 80–90.
- White, D., Fülöp, R., Bishop, P., Mackintosh, A., Cook, G., 2011a. Can in-situ cosmogenic  $^{14}\text{C}$  be used to assess the influence of clast recycling on exposure dating of ice retreat in Antarctica? *Quaternary Geochronology* 6, 289–294.
- White, D.A., Fink, D., Gore, D.B., 2011b. Cosmogenic nuclide evidence for enhanced sensitivity of an East Antarctic ice stream to change during the last deglaciation. *Geology* 39, 23–26.
- Whitehead, J.M., McKelvey, B.C., 2001. The stratigraphy of the Pliocene–lower Pleistocene Bardin Bluffs formation, Amery Oasis, northern Prince Charles Mountains, Antarctica. *Antarctic Science* 13, 79–86.
- Whitehouse, P.L., Bentley, M.J., Le Brocq, A.M., 2012. A deglacial model for Antarctica: geological constraints and glaciological modelling as a basis for a new model of Antarctic glacial isostatic adjustment. *Quaternary Science Reviews* 32, 1–24.
- Wright, A., White, D., Gore, D., Siegert, M.J., 2008. Antarctica at the LGM. In: Florindo, F., Siegert, M.J. (Eds.), *Antarctic Climate Evolution*. Elsevier, pp. 531–570.
- Yamane, M., Yokoyama, Y., Miura, H., Maemoku, H., Iwasaki, S., Matsuzaki, H., 2011. The last deglacial history of Lützow-Holm Bay, East Antarctica. *Journal of Quaternary Science* 26, 3–6.
- Zwartz, D., Bird, M., Stone, J., Lambeck, K., 1998. Holocene sea-level change and ice-sheet history in the Vestfold Hills, East Antarctica. *Earth and Planetary Science Letters* 155, 131–145.